IMPROVEMENT IN QUANTUM YIELD OF VARIOUS QUANTUM DOTS AND THEIR APPLICATION IN QUANTUM DOT LEDs

A DISSERTATION

Submitted in fulfilment of the requirements for the award of the degree

of

MASTER OF TECHNOLOGY

in

ELECTRONICS AND COMMUNICATION ENGINEERING

(With Specialization in Microelectronics &VLSI)

Submitted By

SEVA SADAN

Enrollment No. 17534009

DEPARTMENT OF ELECTRONICS AND COMMUNICATION ENGINEERING

INDIAN INSTITUTE OF TECHNOLOGY ROORKEE

ROORKEE-247667

June-2019

CANDIDATE'S DECLARATION

I declare that the work presented in this report with title "**Improvement In Quantum Yield Of Various Quantum Dots And Their Application In Quantum Dot LEDs "** towards the fulfillment of the requirement for the award of the degree of Masters of Technology in Microelectronics & VLSI submitted in the Dept. of Electronics & Communication Engineering, Indian Institute of Technology, Roorkee, India is an authentic record of my own work carried out during the period from January 2018 to May 2019 under the supervision of **Dr. Brijesh Kumar**, Assistant Professor, Dept. of ECE, IIT Roorkee. The content of this report has not been submitted by me for the award of any other degree of this or any other institute.

DATE: .....

SIGNED: .....
(SEVA SADAN)
17534009
MICROELECTRONICS & VLSI

CERTIFICATE

This is to certify that the statement made by the candidate is correct to the best of my knowledge and belief.

DATE: .....

SIGNED: .....
(Dr. BRIJESH KUMAR)
ASSISTANT PROFESSOR
DEPT. OF ECE, IIT ROORKEE

Acknowledgment

First and foremost, I would like to express my sincere gratitude towards my guide **Dr. Brijesh Kumar, Assistant Professor, Dept. of Electronics and Communication Engineering, IIT Roorkee** for his ideal guidance throughout the period. I want to thank him for the insightful discussion and constructive criticisms which certainly enhanced my knowledge as well as improved my skills. His constant encouragement, support, and motivation were key to overcome all the difficult and struggling phases.

Also, I would like to thank **Aditya Nath Bhatt**, **Medha Joshi, Upendra Kumar Verma, and Varun Kumar Singhal**, Research Scholars, Microelectronics & VLSI, Dept. of Electronics and Communication Engineering, IIT Roorkee for guiding me whenever I faced any difficulty.

I would also thank the **Department of Electronics & Communication Engineering, IIT Roorkee** for providing me the lab and other resources for the project work.

ABSTRACT

The organic LEDs and Quantum dot LEDs can be a better solution that meets both the requirements i.e. Energy efficiency and durability of lighting sources. Quantum dot LEDs are one step ahead from organic light emitting diodes as they can use same quantum dot material to act as emissive layer, for any color combination. In this work fabrication and characterization of the quantum dot light emitting devices (QDLEDs) are carried out. In progress of that firstly quantum dots of different kinds have been synthesized, characterized and treated specifically to improve the quantum yield (QY). For CdSe quantum dots it was improved from 1.52 % to 16.03% while for CdS/CdZnS quantum dots it was increased from 12% to 45%. Characterization of quantum dots includes absorbance measurement, photoluminescence measurement, X-ray diffraction (XRD) analysis, X-ray photoelectron spectroscopy (XPS). Further fabrication of organic light emitting devices (OLEDs) was optimized. This optimized result was used in fabrication of quantum dot light emitting devices (QDLEDs).The blue color CdS/CdZnS quantum dots with 45% quantum yield was use as emissive layer. The electroluminescence of the device closely resembles with the spectra of warm white light.

TABLE OF CONTENT

List of Figures

List of Tables

1. INTRODUCTION AND LITERATURE SURVEY

1.1. Overview

Over the past decades, electronics have entered from its inorganic base to the organic which finds a good pace for research in lighting and display applications. The conventional lighting sources including tungsten light bulb, Halogen lamp, conventional LEDs consume relatively larger electrical energy. Compact fluorescent light bulb (CFLs) being the more energy efficient and longer life is a widely used lighting source at present. But it has its own environmental issues due to the use of mercury[1]. With increasing consumption of electricity for commercial and household usage, the urge for efficient and affordable appliances has surged. Organic LEDs and Quantum dot LEDs can be a better solution that meets both the requirements (i.e. besides being energy efficient it must be highly durable). Consequently, electric appliances have come a long way and have seen drastic changes over a period of time. Thus major factors attracting the researchers in this field are derived from the existing problems which include environmental effects, durability, shortage of power, etc. The solid state light emitting devices use the principle of electroluminescence (EL), which is the result of radiative recombination charge carriers i.e. electron and holes when the external electric field is applied. By increasing the extent of radiative recombination of the injected charge carriers, we can make more energy efficient light sources. The research is now focused in evolving the new materials which are best suited for these devices, procedure to fabricate and to increase the electron and hole mobility for proper recombination in the emissive layer of OLED [2]. The devices have been successfully experimented with organic materials such as small molecules, conducting polymers, etc. as a complementary and/or substitute to the inorganic LEDs. Organic LEDs have distinct advantages of solution processing (low cost), eco-friendly, inexpensive fabrication over flexible. Quantum dot LEDs are one step ahead of OLEDs as it can use the same material (Quantum Dot) to obtain different colored light with better color purity. It is due to fascinating electronic and optical properties of quantum dots.

1.2 Basics of Quantum Dots

Quantum Dots are semiconductor nanocrystals having dimensions typically in between 2-10 nm. Flexible control on optical and electronic properties just by changing the size of nanocrystal semiconductor materials makes them a good class material for the fabrication of different color LEDs. Discretization in energy states due to quantum confinement allows these materials to have controlled narrow bandwidth providing luminescence range from infra-red (IR) to ultraviolet (UV). So these materials are the best-fit materials for the design of energy efficient light sources with better color purity than inorganic semiconductor based sources. The no. of states available is quantified by the ratio of the dimension of the system to dimension (L / a_o) in which one state occupies. In general, L is very large in comparison to (a_o) in bulk materials, so the no. of states so large and narrowly spaced that we assume that the distribution is continuous. When the dimension of the system is of an order of atomic size the no. of states becomes very less in number and we say that it is quantized.

In the bulk system in which all the three dimensions are large, we define the 3D density of states in which energy states in all the three dimensions are assumed to be continuously distributed. The system in which one of the dimensions is made smaller (of the order of atomic size) as in quantum well, the states along that axis are quantized and in the other two directions (plane) it is continuous so we define 2D density of states. Similarly, in quantum wires or nano-wires two dimensions are quantized. In quantum dots energy states in all the three dimensions are quantized and we refer it as 0D material.

In quantum dots, due to three dimensional confinement, there are discrete energy states in the k-space. Finally the consequence is that there are only discrete energy levels, in all the possible k spaces, are allowed[3].

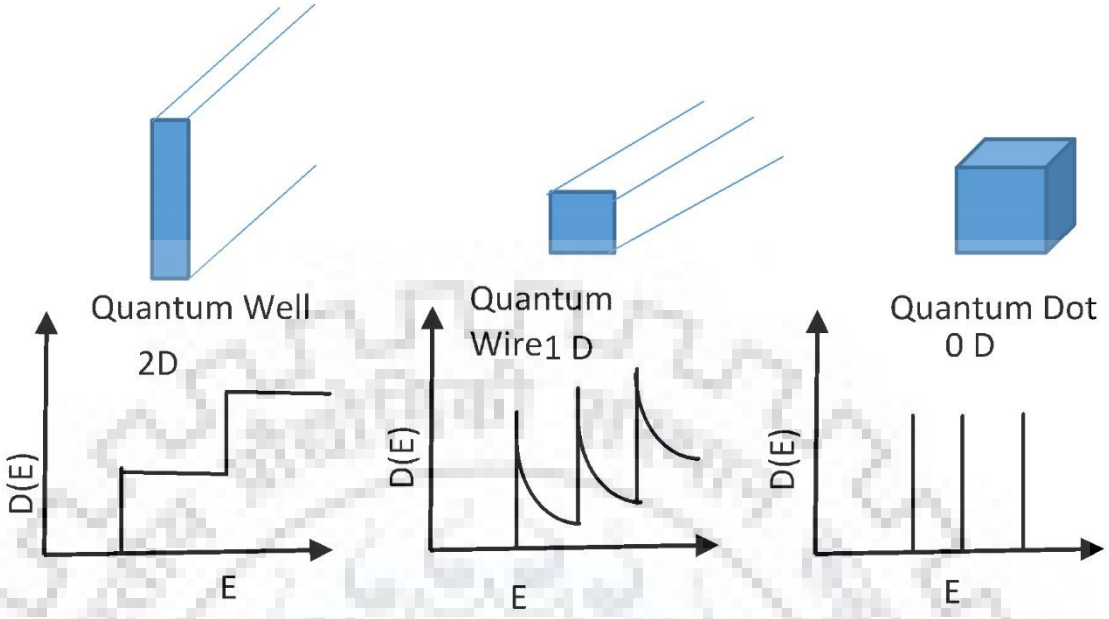

Figure 1.1: Density of states diagram for 2-D, 1-D and 0-D materials

As the size of Quantum dots increases the number of discrete quantized states also increases and thus the energy gap between the HOMO and LUMO of QDs decreases. The wavelength of the light emitted from the QD sample is inversely related to this energy gap Eg, on increasing size Eg increases and in turn wavelength increases. Thus increment in the size of QD results in a shift from blue towards red color.

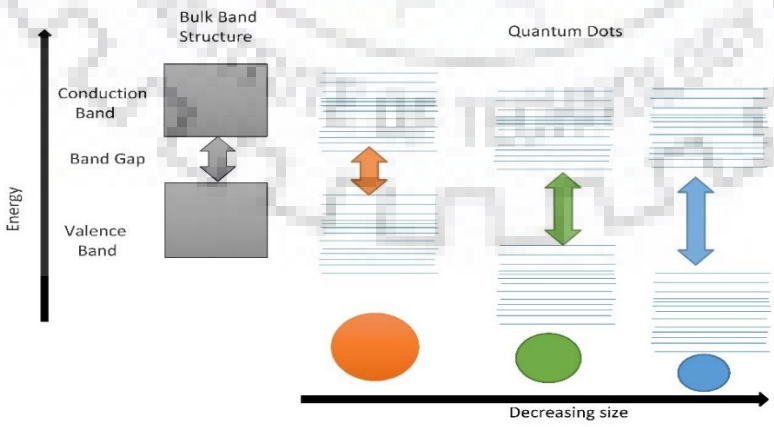

Figure 1.2: Change in energy gap with increasing size of quantum dots

1.2.1 Structure of Quantum Dots

(a) Core Structure

The core structure of quantum dots is composed of about 100-1000 atoms, still allowing discrete energy states. The core structure is characterized by its bandgap which depends on various complicated factors including bond nature, and strength with nearby atoms. Properties lie in between atomic-molecular level and bulk level. In the atomic-molecular level, there are only discrete energy states allowed in which electrons may reside while in bulk materials there are energy bands separated by a bandgap by which decides the nature and application of the material. Thus we can say quantum dots are the combination of two but neither of two. The optical and electronic properties of the quantum dots are associated with this core structure. Figure 1.2 shows the density of states (DOS) of quantum dots (0-D) along with quantum well (2-D) and quantum wire (1-D), it is clear that DOS of quantum dots is delta function of energy, so quantum dots are sometimes described as artificial atoms. Drastic changes in properties such as absorption, exciton energies, electron-hole pair recombination, crystallinity, and impurities are observed when quantum dots size becomes less than ~30 nm of quantum dots. This dependency of properties of quantum dots is associated with quantum confinement effects and variation in surface-to-volume ratio with size.

(b) Surface Structure

The surface structure of quantum dots (QDs) is one of the most important factors in determining their optical properties. Because of being spherical in shape (in general) surface to volume ratio of quantum dots is very high. Studies show that 15% of atoms in CdS quantum dots with size 5 nm are found at surface [4]. These surface atoms have dangling bonds (unsatisfied vacancies) constitutes defect energy states in between the discrete energy states (band gap) of quantum dots energy band diagram, called surface states. These surface states may allow non-radiative recombination of electron-hole pairs. Being high surface area to volume ratio may adversely affect the transfer rate of photogenerated charge carriers. Also, these states are capable of trapping electron or holes and as a result act as an oxidizing or reducing agent. Oxidizing agents are electron deficient species and reducing agents are electron rich. An electron rich defect state is more prone to affect the optical properties such as optical absorption, luminescent intensity, quantum efficiency, optical spectra, and aging effect, as they cannot be reduced by treatment with

an organic ligand. There are proposed methods to convert electron-rich surface defect states to hole rich (i.e. electron deficient) defect states, which can be reduced easily and helps in improving optoelectronic properties of quantum dots. Thus these surface defects need to be passivated to ensure their application in the fabrication of optoelectronic devices.

(i) Surface Passivation

The removal of surface defect states that are created by non-bonded orbitals of surface atoms, is termed as surface passivation. An ideally surface passivated quantum dot has no surface defect states (i.e. all dangling bonds are perfectly saturated) in between the band gap of the energy diagram. This ensures all the near-band-edge states to be quantum confined internally. Practically, it is not possible to achieve the perfectly passivated quantum dot surface. In compound semiconductors, if anionic dangling bonds are left non-passivated, creates defect states just above the valence band. Although, anionic dangling bonds when passivated with available cations results in unsaturated cationic dangling bonds at the surface, which creates defect states just below the conduction band. These cationic dangling bonds can easily be capped or passivated by organic ligands.

Passivation or capping of surface defect states reduces the quenching of radiative recombination of electrons and holes or excitons, thus increasing the quantum yield (QY).

(ii) Organically Capped Quantum Dots

Passivation of cationic dangling bonds can be achieved by capping of organic ligands, which act as Lewis acids. Organic ligands have one or more unbonded electron pairs in excess. In the capping process, one of the electrons from electron pair is transferred to the cationic orbital (dangling bond) and finally, the covalent bond is formed in which both sharing electrons are contributed by the organic ligand itself. Thus organic ligands passivate the cationic dangling bonds through coordination. This type of quantum dots is termed as organically capped quantum dots.

In general, phosphines (e.g., tri-n-octyl phosphine oxide–TOPO) and mercaptans (-SH) are the most commonly used ligands. Organic ligand molecules have definite geometry due to directional properties of covalent bonds, also they form a covalent bond with the cationic vacancy of the quantum dot, thus it is possible that there is a possibility of bond angle bending, which may result in steric hindrance if the organic ligand is bulky in shape

and size. Steric hindrance created by the bulky molecules may lead to cover other nearby sites to be passivated. There is a challenge to passivate both types of dangling bonds (cationic and anionic) simultaneously, so the steric hindrance created may affect the passivation of another type of dangling bond. Also, the same type of organic molecule could not be suitable to passivate both types. Thus the selection of capping agent (i.e. organic ligand) is the critical issue.

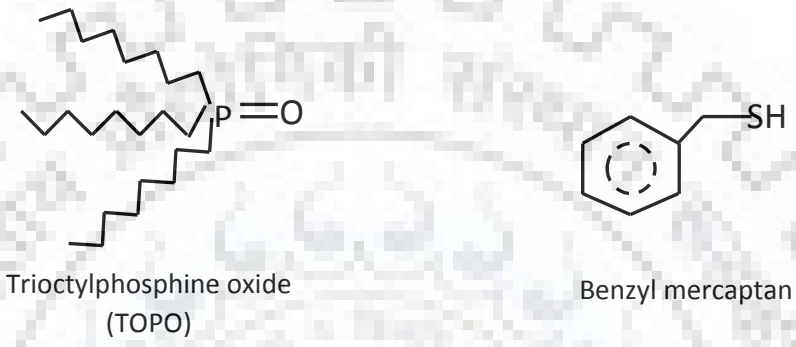

Figure 1.3 Organic ligands used for capping

The organic capped quantum dots are generally photo-unstable. Bonding at the interface between the surface atoms and capping molecules is normally fragile. This results in creation of new surface states when ultraviolet (UV) radiation is exposed over the sample (maybe during characterization) due to passivation failure. The surface states of quantum dots are known to be sites of favored photo-degradation and luminescence deactivation.

(iii) Inorganically Passivated Quantum Dots

Inorganic passivation makes the quantum dots optically stable. This involves shelling of quantum dot core by an inorganic layer of material having a higher band gap than that of the core. Passivation of surface states is done by growing shell over it [5]. This shell may be epitaxial, non-epitaxial, crystalline, or amorphous. During epitaxial growth, the lattice parameters of the shell try to match with that of core material this may cause strain in core/shell structure. As a result of strain generation absorption and emission spectra gets red shifted. Quantum yield of core/shell quantum dots gets increased due to the passivation of surface states of the core by uniform defect free shell coating. Quantum yield also depends on the thickness of the shell coating. If thickens of the shell are increased

much there is a possibility of misfit locations which creates trap states and quenches the radiative recombination of EHP (electron-hole pairs) or excitons. This leads to a decrease in the quantum yield of the core/shell quantum dot. Studies show that the thickness of fewer than two monolayers is sufficient for synthesizing core/shell quantum dots with optimum properties.

1.2.2 Properties of quantum dots

(a) Quantum Confinement Effect

Quantum confinement is a process of restoration of quantization in energy states of the material while moving from macroscopic (bulk crystals) to the microscopic (Nano-crystals) structures. Quantum confinement is said to be established if quantum dot size becomes less than or equal to the exciton Bohr radius. Exciton Bohr radius is the distance between bounded electron and hole (called exciton) by the electrostatic force of attraction, situated far from the nucleus such that they experience a negligibly small force of interaction from it. Exciton Bohr radius is given by the equation as:

$$r_B = 0.0529\epsilon\left(\frac{1}{m_e} + \frac{1}{m_h}\right) \text{ nm} \quad (1)$$

Here,

m_e = effective masses of electron

m_h = effective masses of hole

ϵ = optical dielectric constant

The effective size for quantum confinement to be achieved can also be derived from the de Broglie wavelength and Heisenberg uncertainty principle. Quantum confinement is said to be achieved if the nanocrystal size is comparable to the order of thermal de Broglie wave length($d \sim \lambda_e, \lambda_h$). The exciton energy is a few meV less than that of the band gap and it behaves just like hydrogen atom with a hole as the nucleus. If radius R of the nanostructure approaches to r_B motion of electron and hole wave functions gets confined within the dimension of quantum dot and form standing wave and quantum confinement is achieved [6].

.

$$\lambda_e = \frac{h}{p_e} = \frac{h}{\sqrt{2m_e k_B T}} \quad (2)$$

$$\lambda_h = \frac{h}{p_h} = \frac{h}{\sqrt{2m_h k_B T}} \quad (3)$$

According to the Heisenberg Uncertainty principle, uncertainty in the momentum of a particle with dimensions′ having mass m is given by-

$$\Delta p \sim \frac{\hbar}{d} \quad (4)$$

The confinement along the specified direction causes the kinetic energy to increase and is given as-

$$E_{confinement} = \frac{(\Delta p)^2}{2m} \sim \frac{\hbar^2}{2md^2} \quad (5)$$

This additional increment in kinetic energy must be greater than or equal to the kinetic energy in particle-associated due to the thermal motion. That is,

$$\frac{\hbar^2}{2md^2} \geq k_B T \quad (6)$$

Thus the maximum size of the nano-crystal to achieve quantum confinement can be expressed as-

$$d \approx \frac{\hbar}{\sqrt{2mk_B T}} \quad (7)$$

There are two proposed theoretical models to understand the quantum confinement namely (i) Effective Mass Approximation Model (ii) Linear Combination of Atomic Orbital Theory

(i) Effective Mass Approximation Model

The effective mass approximation model was proposed by *Efros* and *Efros* in 1982 used to model the prediction of quantum confinement. This model deals under two conditions $R \geq r_B$ and $R \leq r_B$. This is an idealized model, based on the 'Particle-in-Box Model' with the infinite potential well at crystal surface which excludes the coulombic interaction. *Efros* and *Efros* made some assumptions such as bands to be a parabolic and infinite potential barrier [7] [8] at the microcrystalline surface. Hamiltonian operator to govern this confinement problem is given by-

$$H = -\frac{\hbar^2}{2m_e^*}\nabla_e{}^2 - \frac{\hbar^2}{2m_h^*}\nabla_h{}^2 + V(r_e) + V(r_h) - \frac{e^2}{\varepsilon_2(r_e - r_h)} \quad (8)$$

This equation can be analyzed in 3 regimes as-

(a) Weak confinement regime ($R >> r_B$): Here, only motion of center of mass of the excitons is quantized, this doesn't affect their relative motion. The quantization energy is given, in the above approximations of a spherical dot having infinitely high energy barriers and neglect the difference of the dielectric properties microcrystalline structure and the surrounding, by (here $M = m_e + m_h$) -

$$\Delta E_Q = \frac{\hbar^2\pi^2}{2MR^2} \quad (9)$$

(b) Medium confinement regime ($r_e > R > r_h$): In this regime, the motion of the electron is quantized while that of hole is not. The holes move in the potential created in quantum dot and of the space-charge of the electron for the usual condition of $m_e << m_h$.

Assuming the stated conditions and neglecting the columbic interaction energy between electron and hole, we get-

$$\Delta E_Q = CR_y{}^* \left(\frac{\pi r_B}{R}\right)^2 ; C = 0.67 \quad (10)$$

$R_y{}^*$ is Rydberg energy

(c) Strong confinement: In this regime the exciton energy is very-very high in comparison to columbic interaction between the same pairs and is given as-

$$\Delta E_Q = \frac{\hbar^2\pi^2}{2\mu R^2} \gg E_{coulombic} \quad (11)$$

Here μ = Reduced mass of electron and hole, smaller than both the carriers' masses.

(ii) Linear Combination of Atomic Orbital Theory–Molecular Orbital Theory

Molecular orbital theory tells that all the orbitals from valence shell to lowest energy shell take part in bond formation in contrast with the valence bond theory which deals only with valence shell orbitals. When two atomic orbitals linearly combine their wave functions superimpose in either constructive fashion or destructive fashion. In constructive fashion

(same phase) of overlap, the probability of electron confinement $|\psi|^2$ increases thus decreasing the energy, this newly formed orbital is called bonding molecular orbital (BMO) while in destructive case energy of the orbital increases and is called ant-bonding molecular orbital (ABMO).

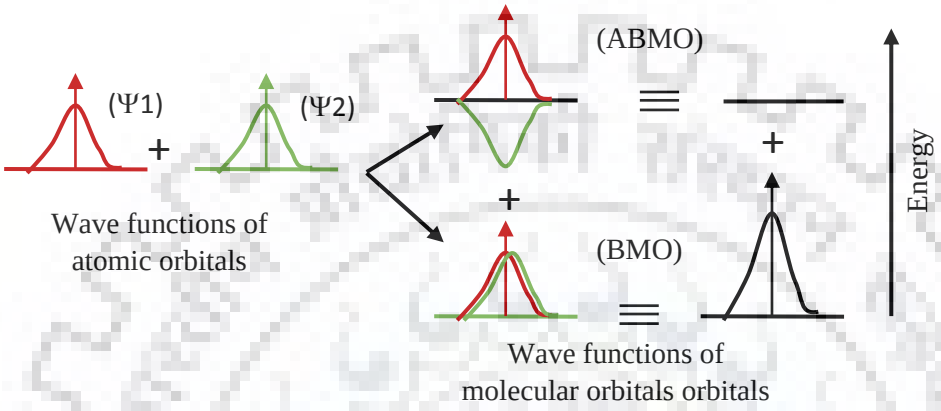

Figure 1.4: Linear combination of atomic orbitals

The number of newly formed molecular orbitals is equal to the number of atomic orbitals taken part in the chemical combination process. Clearly, the energy of bonding molecular orbitals (BMO) is lesser than that of anti-bonding molecular orbitals (ABMO). These are the energy states, in which charge carriers can now reside. When a large number of atoms come to combine with each other to form a crystal, their all atomic orbitals overlap, depending upon their degree phase of overlap their energy gets split into bands namely valence band and conduction bands. The separation between the two bands is called the energy gap (Eg). When the number of atoms to combine is lesser (between 100 to 1000) the linear combination of atomic orbitals results in the formation of discrete energy states BMOs and ABMOs. The unoccupied ABMOs are called as lowest unoccupied molecular orbital (LUMO) levels and occupied BMOs are called as highest occupied molecular orbital (HOMO) levels. The gap between the highest energy level of the LUMO level and the lowest energy of the HOMO level (energy gap) decreases as size increases. It is due to further mixing of orbitals which results in an increase in the highest energy of the LUMO level and a decrease in the lowest energy of the HOMO level.

Thus we can say that quantum dots structure and electronic properties lie in between that of atoms/molecules and bulk crystals. This model provides a methodology to explore the electronic properties quantitatively for very small quantum dots, for large size quantum dots it gets failed due to complex mathematics and limitation of computing systems. However, the extent of quantum confinement is quantified by the ratio of quantum dot radius to the Bohr exciton radius (r_B).

(b) Luminous Properties

Luminous property of quantum dots is associated with the emission of radiation in the visible region of the spectra. It is due to the energy gap value which lie in between the atomic/molecular discrete energy gap and the band gap in bulk materials. When the QDs are excited with external source, electron goes from LUMO level to HOMO level and when it gets deactivated, emits electromagnetic radiation. Deactivation of electron and holes or excitons can be either radiative (emit photons) or non-radiative (emit phonons or Auger electrons).Non-radiative emission in quantum dots is mainly due to presence of trap states in between the discrete energy states of the material. The possible types of deactivation (relaxation modes) are explained below.

(i) Radiative Relaxation

In radiative relaxation, there is self-luminescence comes out from the quantum dots (QDs). This luminescence is result of either band-edge or near band-edge transitions or from defect quantum energy states.
These emissions are discussed below-

(ii) Band-Edge, Near Band Edge and Defect State Emissions

Band edge and near band edge emissions are the results of the radiative relaxation processes in intrinsic semiconductors. When a conduction band electron gets recombined with the valence band hole it results in band edge emission. It is possible that electrons and holes get bounded to form excitons whose energy is slightly lower than the band gap, when they recombine radiatively is called near band emission.

When an excited electron gets transition through defect states and finally recombine with the hole of valence band this is called defect state or trap state emission.IT may or may not be radiative.

1.2.3 Synthesis of Quantum Dots

(a) Wet chemical method

It is one of the most popular methods to synthesize quantum dots. The following two categories are mainly focused on this synthesis method.

(i) Aerosol Based Synthesis

In this method, a colloid of liquid droplets in the gaseous precursor is formed to produce the desired quantum dot, which is called aerosol. Liquid droplets are the liquid precursors used. The concentration of precursor and size of the aerosol droplets determine the size of the quantum dot.

(ii) Solution-Based Synthesis

In this method, two solution based precursors are used and they are mixed together to take part in the chemical reaction. Reagents are added to the solution such that its concentration and timing determine the size of a quantum dot formed.

(b) Vapor phase method

In the vapor-phase synthesis of the quantum dot are fabricated in those conditions, where the vapor phase mixture is comparatively unstable with thermodynamics point of view, thus preparation of solid material is not preferred. Then it is condensed to get from quantum dots. This technique mainly depends on the condensation process.

1.2.4 Characterization of Quantum Dots

Characterization of quantum dots can be categorized in two sections optical characterization and structural characterization

(a) Optical characterization

Optical characterization includes the measurement of absorbance, photoluminescence, and quantum yield.

(i) Absorbance spectra

Absorbance is defined as the amount of light component absorbed by a sample when a homogeneous source of light falls over it. When a light source containing a wide range of wavelengths is allowed to fall over the quantum dots solution, it absorbs the entire spectra below a certain wavelength. This maximum wavelength is the wavelength corresponding to the absorption peak. The beginning of absorbance indicates the wavelength matching to the band gap of the quantum dots.

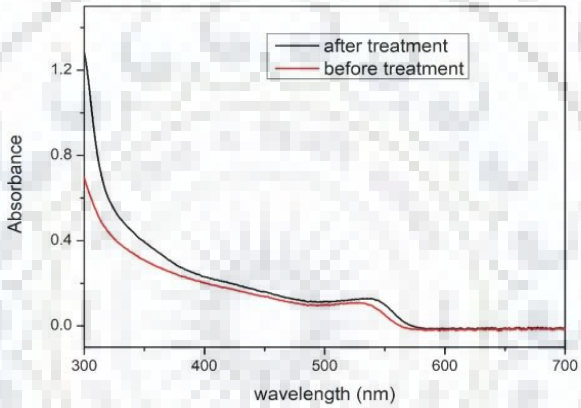

Figure 1.5: Absorbance spectra of CdSe quantum dots

Organic compounds with conjugated π-systems are referred to as Organic semiconductor materials. These are the polymers consisting of carbon skeleton along with hydrogen and other hetero-atoms such as nitrogen, sulfur, oxygen, etc. These are basically electrical insulators with a typical band gap of 2.5-4eV which is larger than the band gaps of inorganic semiconductors, which is typically 1-2eV, they become semiconducting when charges are injected (i) from appropriate electrodes (ii) through doping (iii) by photo-excitation [3]. These materials show intense and broad absorption. As the thickness of the organic semiconductor used in the fabrication of light emitting devices is kept very small, the incident light is not captured significantly. The absorption can be increased by having an ordered solid crystalline structure. Also, dyes can be used to improve the absorbance if needed.

Absorbance also depends on the key functional groups attached to the carbon skeleton. They shift the maxima of absorbance spectra to the larger wavelength. The absorbance characteristic of a quantum dot is shown in Figure 1.5 It shows that the sample is capable of absorbing light having a wavelength lower than 550 nm.

(ii) Photoluminescence (PL) Spectra

It is defined as the emission of light from any matter after absorption of electromagnetic radiation (photon). PL of any material is shifted to a larger wavelength with respect its absorbance spectra, this is called Stokes Shift. The reason for Stokes shift is the availability of a large number

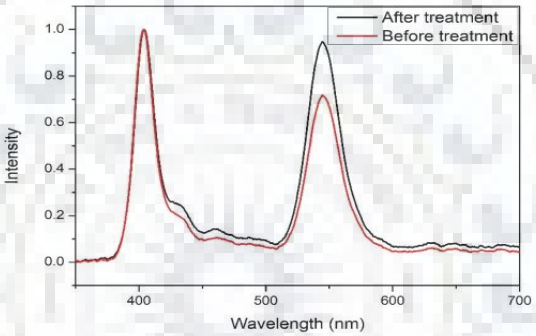

Figure 1.6: PL of CdSe samples after and before treatment with $NaBH_4$

of transition states ($nC2$: if an electron is excited from ground to nth excitation state) with lower energy differences (ΔE) with equal probability to be occupied by an electron making transition. As the wavelength of the emitted photon is inversely proportional to the ΔE, the wavelength of emitted photons increases. The Figure 1.6 also shows the PL of a general sample in. The first peak comes at 550 nm which corresponds to the maxima of emission spectra. It is interesting to observe that the PL spectra of the quantum dot are confined within a very narrow wavelength range, it is due to the fascinating property of quantum dots to have wide absorption spectra, but fine emission spectra.

Upon exciting the quantum dot using a reasonable monochromatic light source, the quantum dots show the phenomenon of photoluminescence in which the photons of some wavelength are emitted when electrons are excited with some light source. The figure clearly shows the emitted spectra when quantum dots are excited with the light

source whose spectra are shown alongside. The full-width half maxima (FWHM) is a good measure of uniformity of the size of nanoparticles. Due to the small size of QDs (lesser than exciton Bohr's radius), the discrete energy levels are sufficiently far apart to significantly reduce the probability of electron transition in levels other than the ones right at the edge of the bands. Smaller the FWHM, better is the uniformity.

(iii) Quantum Yield

It is defined as the ratio of the count of the photon emitted to the count of photon incident over the quantum dots.

QY=No. of absorbed photons/No. of emitted photons

(b) Structural Characterization

There are different measurements that are carried out to know the structure of the QD, their composition, size, etc.

(i) X-ray Photoelectron Spectroscopy (XPS)

XPS is a surface sensitive spectroscopy technique that is used to know the chemical composition of the crystal surface of any electronic material or crystal. The determination of composition is based on two principals one of them is the photoelectric effect and the rest one is different chemical bond possesses different bond energies. The sample is irradiated with the X-ray beam and kinetic energy of ejected electrons from the surface is quantified and the number of electrons ejected, corresponding to different bond ionizations resulting in a different energy, are counted. XPS survey scan of the CdSe quantum dots is shown below:

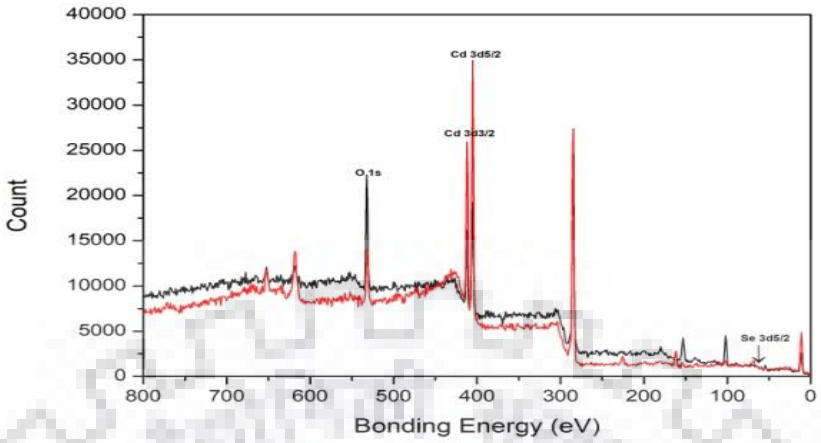

Figure 1.7: XPS survey scan of two different CdSe quantum dots

(ii) X-ray Diffraction (XRD) Analysis:

It is used to know the crystal structure or the identity of the crystalline material. The x-ray diffraction pattern is formed when the X-rays imposed over the crystalline material gets reflected from the different crystalline layers and interfere constructively. The Scherer's formula-

$$d = 0.94\lambda / B\cos\theta \qquad (12)$$

Where,d = Average crystal size, λ = wavelength of the X-Ray used, B= FWHM

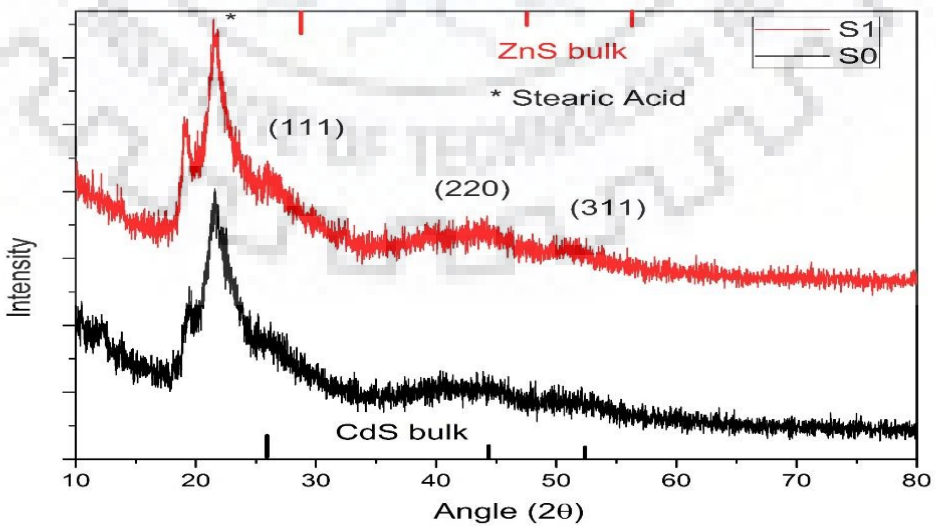

Figure 1.8: XRD of CdS/CdZnS blue quantum dots

of the peak in XRD pattern, θ = Bragg's angle of reflection. A diffraction pattern is characterized by its peak position, peak

intensity, and peak width. Peak intensity depends upon the size and shape of the unit cell of the crystal. The number of atoms and position of atoms in the unit cell determines the peak intensity and peak width depends upon instrumental parameters, crystal size, temperature strain, and inhomogeneity. The different peaks in the pattern account for the different materials present in the thin film of dispersed solution or powder. The XRD pattern of the CdS/CdZnS core-shell structure is shown in the figure below.

(iii) Transmission Electron Microscopy (TEM)

It is used to know the shape and size of the nano-crystals. Its functioning is based on the simple concept of magnification of a thin film of a crystal by a high-resolution transmission electron microscope. It uses a beam of electrons instead of light thus exploiting the wave-particle duality. The electron beam is produced, accelerated and focused, by electronic lenses in an electron gun, on the sample. The beam passing through the sample impinges the image which is further magnified by the high-resolution microscopes and detected by using fluorescence. TEM images of two different CdSe quantum dots are shown below.

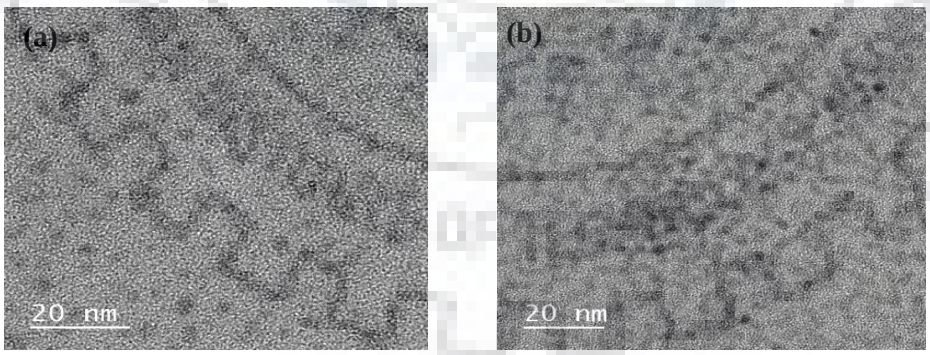

Figure 1.9: TEM images of CdSe Quantum Dots

1.3 Organic light emitting Devices(OLEDs)

1.3.1 Structure of OLEDs

To improve the device performance which depends on the various factors including electronic property of material layer, thickness of the layer, fabrication environment, and physics associated with the charge balance, etc. The basic structure may contains emissive layer sandwiched between anode and cathode. More advance devices contain electron transport layer (ETL), hole transport layer(HTL) along with anode and cathode to facilitate the carrier transport.

Multilayer structure basically has the following layers:

(a) Substrate
(b) Anode
(c) Hole Injection Layer(HIL)
(d) Hole Transport Layer(HTL)
(e) Emissive Layer (EL)
(f) Electron Injection Layer(EIL)
(g) Electron Transport Layer(ETL)
(h) Cathode

The substrate is the base of the device which must be transparent (for bottom conducting devices) to allow the emitted light to pass. It generally works as an anode that's why it must be conducting also. It consists of a glass base over which conducting transparent material is deposited. It also provides mechanical strength to the device against wear and tear. For flexible OLEDs, flexible substrates are proposed. ITO (Indium tin oxide) is the commonly used material for anode due to having very low surface roughness and high work function. It is observed that a rough anode surface results in a short circuit in the device, so, an optimum level of surface roughness is only allowed for the proper functioning of the device. Hole injection layer allows the injection of holes into the device when external energy source (Voltage or current source) is applied. So its LUMO level should not be much higher than that of the anode. The hole transport layer (HTL) further supports the transportation of hole. Actually, a multilayer structure with a very small gradient in the LUMO level increases the hole conductivity. While using ITO as anode we generally use PEDOT: PSS (poly(3,4-ethylene dioxythiophene) polystyrene sulphonate) as

HIL (hole injection layer) and PVK as hole transport layer (HTL). The electron injection layer (EIL) allows the injection of electrons from the cathode end electron are supported by EIL and ETL layers to reach the emissive layer (EL). In emissive layer electron and hole recombine forming exciton and finally deactivate radiatively and produces light of color decided by the band gap of the emissive material and its photoluminescence (PL). A solution processed layer formation is preferred because of ease of synthesis, this allowed chipper and lesser fabrication time for synthesis. A blending of HTL and EL layers are proposed to do so also it may result in better efficiency. For example PVK a hole transport layer (HTL) and Alq3, an emissive layer (EL) can be blended. This reduces one step i.e. thermal deposition of alq3 which is a more costly and time-consuming step.

OLEDs can further be classified, based on the material used for anode and cathode, as:
(a) Top Emitting OLEDs

(b) Bottom Emitting OLEDs

Clearly, the emitting side of the OLED should be transparent to the emitted photon so as to allow the light to come out of the device. The cathode is generally a low work function material allowing the easy injection of electrons into the stack of layers. Sometimes, more than one layer of the cathode is deposited to smoothen the barrier step to facilitate the electron injection eg. Li: Al.

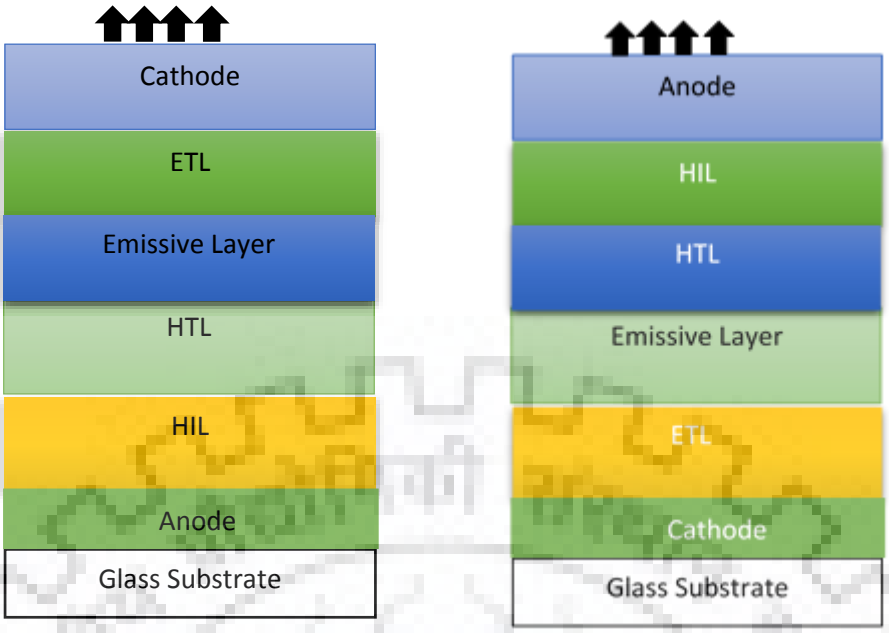

Figure 1.10: TOP emitting OLEDs

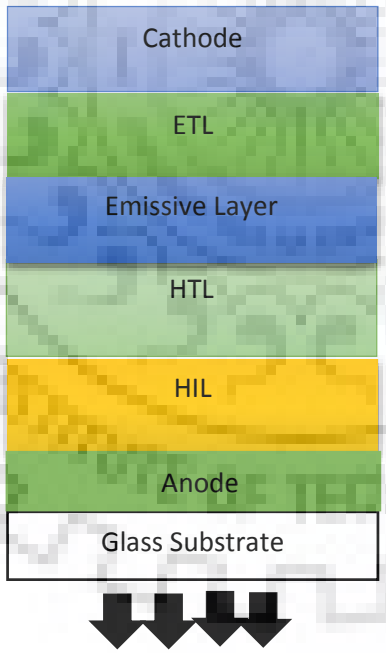

Figure 1.11: Bottom emitting OLEDs

1.3.2 Materials used in the fabrication of OLEDs

Organic LEDs require different materials for different layers. The selection of material depends on their electronic properties (band step requirement, bang gap and/or work function etc), structure of the device (Bottom or Top-emitting), ease of fabrication mobility of carriers in the material so as to allow injection of electrons and holes from cathode and anode terminals with least barrier. The number of layers is allowed to control the mobility of the injected carriers that is electrons and holes for example layer of materials whose LUMO levels differ by very small value supports in increasing the hole mobility. However, researchers have used the following materials for the different layers. The details of the materials have been shown in the table 1.

Table 1: List of materials used in fabrication of OLEDs

Sr No.	Layers of OLED	Suitable Materials
1	Anode	ITO(4.7eV),ZnO(5.07eV), Au(4.26eV), Pt, Ni etc.
2	Cathode	Mg: Ag, Li: Al, Ca, etc.
3	HIL	CuPc, TPD, NPB, PVK, PPV etc.
4	ETL	Alq_3, $Bebq_2$, BCP, TAZ, etc.
5	EL	Alq3, nanoparticles, etc.

1.3.3 Principle of operation

Light emitting devices work on the principle of electroluminescence, which is defined as the one in which the luminescence is observed when an external electric field is applied across the device. This phenomenon is facilitated by the advanced band alignment engineering in the stacked device structures. Unlike incandescent in which light is emitted

due to the glow occurring due to the sufficiently high temperatures commonly referred as hot light as in the case of celestial stars, luminance occurs due to the settling of electrons from high energy states to the lower ones. Basically, an excitation is required before the settling, which is accompanied by energy transfer through the electric field, to take place resulting emission of light. On the basis of excitation (commonly termed as radiation), luminance is mainly of following types namely:

(a) Electroluminescence

(b) Fluorescence

(c) Phosphorescence

In electroluminescence, electric field is used to excite the electrons from lower energy state to higher energy state, which on relaxation release photons of wavelength equivalent energy and produces luminescence. Similarly, if electromagnetic radiations such as UV, X-ray, etc. are used as a source of excitation, this process of the emitting photon is called fluorescence. Phosphorescence differs with fluorescence in its photon emission mechanism. The excited electrons in the case of phosphorescence have delayed relaxation due to the presence of traps on their way back. This delayed relaxation can lead to a shift in the original wavelength supposed to be emitted earlier.

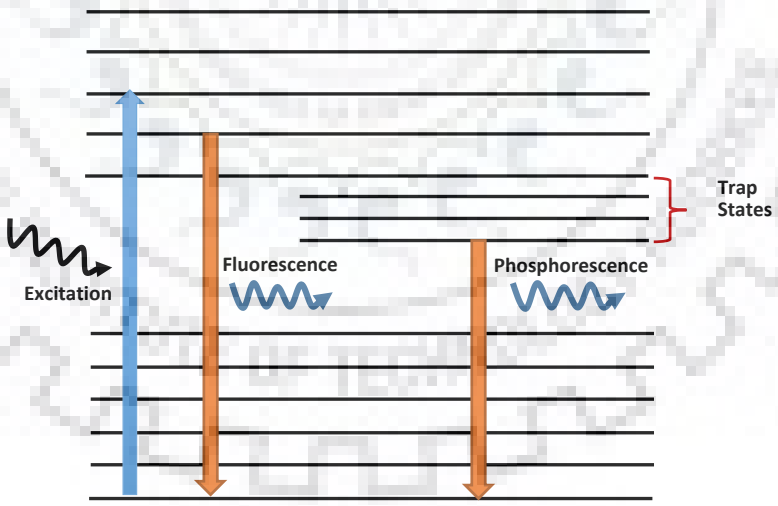

Figure 1.12: Showing Fluorescence and Phosphorescence

In case of organic light emitting devices, organic layers are engineered such that they allow the injection and transport of charge carriers of opposite nature in opposite direction to finally meet at the junction to emit the light corresponding to the band gap of the emissive layer material. This happens upon the application of the electric field of the

desired polarity across the electrodes, a phenomenon known as electroluminescence as discussed above.

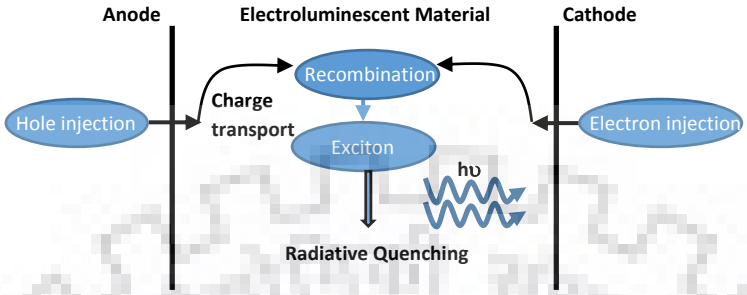

Figure 1.13: Showing electroluminescence

1.3.4 Fabrication of OLEDs

Fabrication of Organic Light Emitting Devices (OLED) involves simple processes including Substrate preparation, Fabrication (deposition of different organic and metallic layers) and Packaging. The fabrication flow of the OLEDs is shown in the figure below.

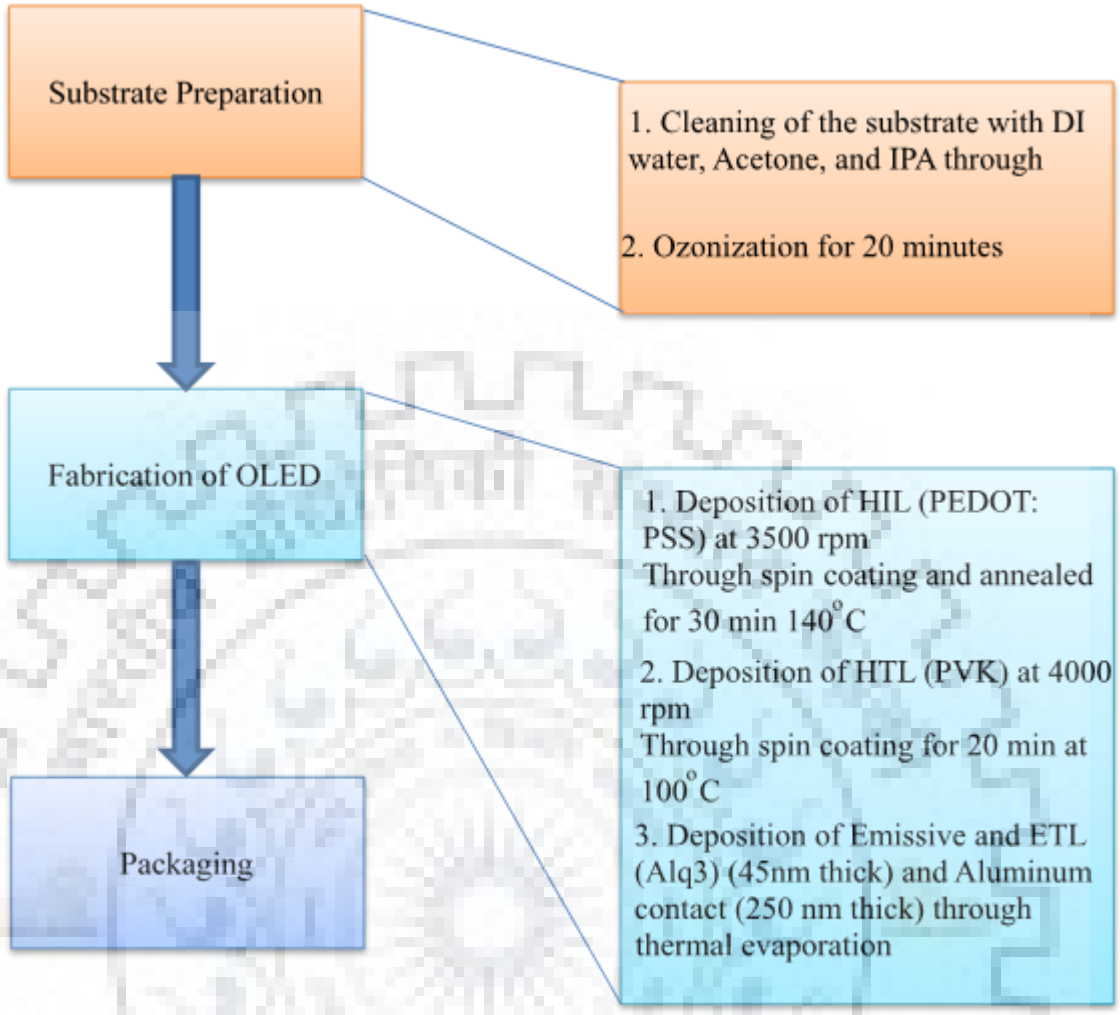

Figure 1.14: Fabrication flow of OLEDs

1.4 Quantum Dot Light Emitting Devices (QDLEDs)

1.4.1 Structure

Quantum dot LEDs structure is the same as that of the OLED except for the emissive layer which is a layer of quantum dots.

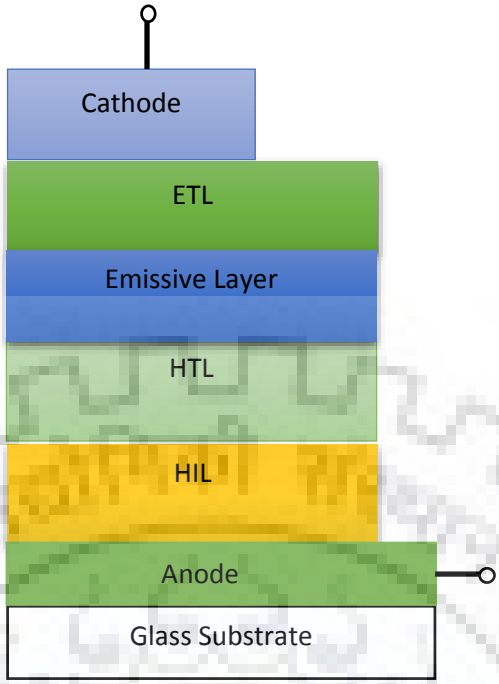

Figure 1.15: Structure of QDLEDs

1.4.2 Fabrication QD LEDs

The fabrication process of the QDLEDs is the same as that of OLEDs. The material selection for different neighboring layers is decided by HOMO and LUMO levels of quantum dots so that they support the transmission of one type carrier and blocking of other so that they can recombine in the emissive layer.

1.5 Electronic transport in OLEDs and QDLEDs

In OLEDs and QDLEDs when the external energy source is applied it forces to in injecting holes from the anode (ITO) and electrons from cathodes (Al). Injected holes follow the gradient of LUMO levels of the HIL and HTL layers and reach to emissive layer (QD layer in QDLEDs), on the other hand, injected electrons follows the gradients of HOMO levels of the EIL and ETL layers and reaches to the emissive layer. Higher HOMO of the HTL and Lower LOMO of the ETL supports in blocking the electrons and holes respectively to cross the emissive layer. These electrons and holes come together and form excitons further these excitons get quenched radiatively, thus emitting the light of the desired color. In quantum dots, the color of the emitted light (Electroluminescence)

depends upon the band gap (Eg) of the QD material as well as the photoluminescence property of QD.

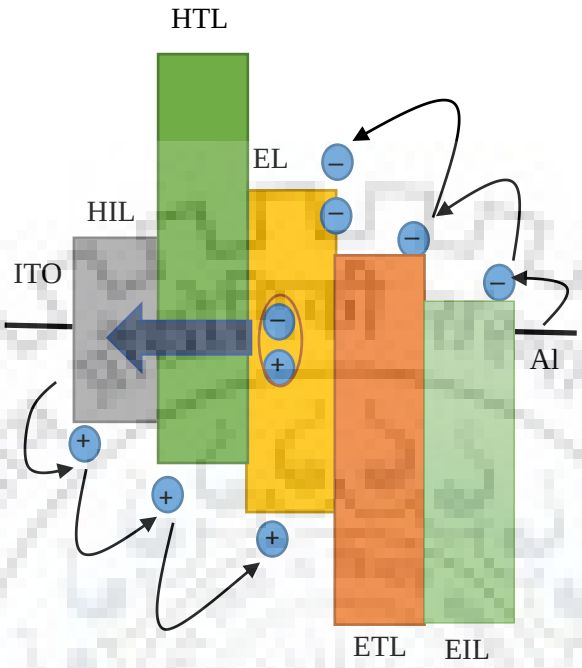

Figure 1.16: Light Emission in OLEDs and QDLEDs

1.6 Structure of the dissertation

Chapter2 includes the synthesis and characterization of green CdSe core quantum dots, improvement in quantum yield by conversion of Se surfactants rich QD to Cd surfactant rich by the simple method of surface treatment

Chapter3 includes improvement in quantum yield (QY) of blue color CdS/CdZnS core/shell quantum dots.

Chapter4 consists of the fabrication and characterization of green color organic light emitting devices (OLEDs) and hot white color quantum dot light emitting devices (QDLED).

Chapter5 consists of the conclusion of the work and future scope.

2. CONVERSION OF Se-RICH TO Cd-RICH SURFACTANTS: ENHANCEMENT IN QUANTUM YIELD (QY) OF TRIOCTYLPHOSPHINE (TOP) CAPPED CdSe QUANTUM DOTS (QDs)

The semiconductor quantum dots (QDs) are the nanoparticles with typical dimensions ranging from 1-10 nm [1]. Low-cost solution-based synthesis, tunable emission, flexible control on optical and electronic properties just by changing the size make QDs suitable for potential application in the photovoltaic, light emitting diodes (LEDs), and lasers [9]. Discretization in energy states due to quantum confinement allows these materials to have controlled narrow bandwidth providing luminescence range from infra-red (IR) to ultraviolet (UV). So, these are the best-fit materials for the design of energy efficient organic light sources with better color purity than inorganic semiconductor based sources.

Besides this, these materials suffer from their poor stability and low quantum yield. Defect states present in the bulk as well as on the surface creates trap states in between the discrete energy states of QDs that cause non-radiative recombination. Se surfactants are anionic sites and Cd surfactants are cationic, both constitute defect states in between the discrete energy states of QD. Being electrophilic in nature, QD with Cd surfactants can easily be coordinated with organic ligands (electron rich species) and atmospheric oxygen. While in the case of Se rich surfactants, being electro phobic in nature, the coordination with organic ligands and oxide ions is not possible. There is a possibility of formation of SeO_2 through back bonding with vacant d-orbitals of Se, but this does not reduce the defect state created due to anionic sites. Thus conversion of Se rich QD to Cd-rich QD allows a better degree of passivation by organic ligands and atmospheric oxygen [10][11].

In this work, freshly prepared CdSe quantum dots were surface treated with reducing agent NaBH4 to convert the Se rich CdSe QD to Cd-rich QD with tenfold increment in quantum yield (QY). Different measurements including absorbance, photoluminescence quantum yield (QY), XPS, X-ray thin film diffraction (XRD) patterns, and FLS are performed to justify the results.

2.1 Materials used

Cadmium oxide (CdO), Selenium powder (Se), Oleic acid (OA), 1-octadecene (ODE), and Trioctylphosphine (TOP), Sodium borohydride (NaBH4), all these materials were purchased from Sigma-Aldrich. Acetone and chloroform used were of spectroscopic grade.

2.2 Synthesis of CdSe QDs

The CdSe QDs were prepared by following the methods of the reference papers [12] and [11] with slight modifications. The CdSe quantum dots have been synthesized by mixing the freshly prepared Cd and Se precursors at a specific temperature. Selenium precursor was prepared by mixing 0.020 gm Se and 0.1 ml TOP in 2 ml 1-octadecene, and stirring for one hour. The mixture of 0.102 gm CdO, 14 ml 1-octadecene, and 1.2 ml oleic acid are taken in a 100 ml round neck flask and heated with simultaneous stirring at 180˚C under N_2 environment. When the solution of cadmium oleate ($Cd(OA)_2$) formed becomes clear, the temperature is increased to 220˚C. At this point, 2 ml of freshly prepared selenium precursor is quickly injected. After the injection of the Se precursor, the QD sample is taken after 60 s. The freshly prepared QDs are divided equally into two parts. First, a part is kept intact and abbreviated as sample S0 while the second part is mixed with NaBH4 solution (4% W/W) and stirred for about 2 hours at 500 rpm, named as sample S1. Further, the CdSe quantum dots are purified by mixing it with chloroform and acetone in the ratio 1:1:3 and centrifuging at 6000 rpm for about 10 minutes.

2.3 Characterization

The X-ray thin film diffraction (XRD) patterns of thin film CdSe QDs were recorded using Bruker, D8-Advance XRD system. Ultraviolet-visible absorbance spectra of CdSe QD samples were recorded with a USB: 4000 ocean optics spectrometer assembly. Steady-state photoluminescence (PL) were collected on USB: 4000 ocean optic spectrometer, an LED source (373 nm, FWHM~15 nm) was used as a source of excitation. The quantum yield (QY) of the samples was measured using the integrating sphere equipped with an LED source (373 nm, FWHM~15 nm) and USB: 4000 Ocean spectrometer assembly. X-ray photoelectron spectra were captured on an X-ray photoelectron spectroscopy (XPS) instrument (Physical Electronics, Model-PHI 5000 Versaprobe III) assembled with a monochromatized Al k-α X-ray source (hυ=14866.6 eV) as a source of excitation. All binding energies were calibrated with respect to the C1s peak (285.0 eV) present in all spectra taken as a standard. Time-correlated single photon counting curves

(TCSPC), to measure the lifetime of QDs, were obtained using Fluorescence Lifetime Microscope (HORIBA JOBIN YVON Model- FLUOROCUBE), consisting of nano LEDs with wavelength 373 nm as source of excitation, fluorescence detection range 300 – 800 nm (using TBX-04D detector) and Emission Monochromator of range 200 – 850 nm with varied bandwidths ranging from 1-32 nm in different steps.

2.4 Results and Discussion

The absorbance and PL characteristics of QD samples S0 and S1 are shown in Fig. 1. First absorption peaks for samples S0 and S1 shown in left are obtained at wavelengths 467.60 nm and 468.06 nm respectively. Particle size estimated, from the theoretical equation [13] by using the measured wavelengths of first absorption peaks, for samples S0 and S1 are found to be 1.98 nm and 2.08 nm respectively as tabulated in Table 2.2. This increment in the size of QDs of sample S1 also depicted in PL spectra whose emission maxima is red shifted by 10 nm as shown in Fig. 1 (right). This increment in size (~1A^{o}) is approximately

Table 2.1: PL peaks, size, FWHM, Quantum Yield and average lifetime measured at room temperature

Sample	λ_{em} (nm)	Size (nm)	FWHM (nm)	QY (%)	τ_{av}(ns)
S0	549.76	1.98	31.96	1.52	2.21
S1	559.80	2.08	31.83	16.03	6.16

Table 2.2: Stoichiometry and surface atomic ratios of QD samples S0 and S1

Sample	Cd_s/Cd_{inn}	Se_s/Se_{inn}	Atomic Percentage		
			Cd	Se	O
S0	0.69	Very High	17.85	2.01	80.14
S1	0.75	1.37	48.93	0.18	50.89

the same as the ionic size of Cd^{++} (~0.95A^{o}) [14].

This proves that there is the bonding of Cd^{++} ions with anionic facets present at the surface of CdSe QD when XRD of the CdSe QD sample is treated with NaBH4, thus now anionic facet rich QD is converted into cationic facet rich as shown in Figure 2.3. This cationic facet rich QD gets passivated easily with atmospheric oxygen forming an oxide and with TOP forming TOPO. The greater degree of passivation is provided for the surface treated sample S1 (having a cationic rich native) than sample S0 (having anionic rich native) [10]. This decreases non-radiative surface states thus increasing QY of S1 approximately 10 times than that of S0 at the cost of ~1A^o increment in size as shown in Table 2.1.

Also, PL spectra of samples S0 and S1 show the narrow band edge emission (FWHM<40nm) and a lower energy trap related emission. The quantum yield of samples S0 and S1 were found to be 1.5 % and 16.01 % respectively. Thus, surface defects dominate in both the samples including dangling bonds of Cd and Se act as cationic and anionic facets respectively. The XRD patterns of QD samples S0 and S1 are shown in Fig. 2. The pronounced peaks corresponding to the plane (111) are the characteristics of the zinc blende phase structure of CdSe [15].

The fluorescence lifetime of the quantum dots was measured using a time-resolved Fluorescence lifetime measurement setup (Horiba Jobin-Yvon, model-Fluorocube) at an excitation wavelength of 373 nm. Lifetime measurement is done by fitting the plot with a triple exponential function given by (13).

$$I(t) = A_1\exp(t/\tau_1)+A_2\exp(t/\tau_2)+A_3\exp(t/\tau_3) \quad (13)$$

Here A_1, A_2, A_3 are pre-exponential factors and τ_1, τ_2, and τ_3 are corresponding lifetimes. The average life (τ_{av}) is obtained as the weighted average of τ_1, τ_2, and τ_3 given in equation (14)[9].

$$\tau_{av} = (\tau_1 A_1+\tau_2 A_2+\tau_3 A_3)/(A_1+A_2+A_3) \quad (14)$$

The average life time of S1 (6.16 ns) is found about 3 times greater than that of S0 (2.21 ns). The average lifetime is the function of radiative recombination rate (k_r) and non-radiative recombination rate (k_{nr}) as expressed in equation (15) [16].

$$\tau_{av} = 1/(k_r+k_{nr}) \quad (15)$$

This increment in the average lifetime of sample S1 is due to decrement in the value of non-radiative recombination rate (K_{nr}) thus after surface treatment with NaBH4 the number of non-radiative sites has been decreased to a large extent.

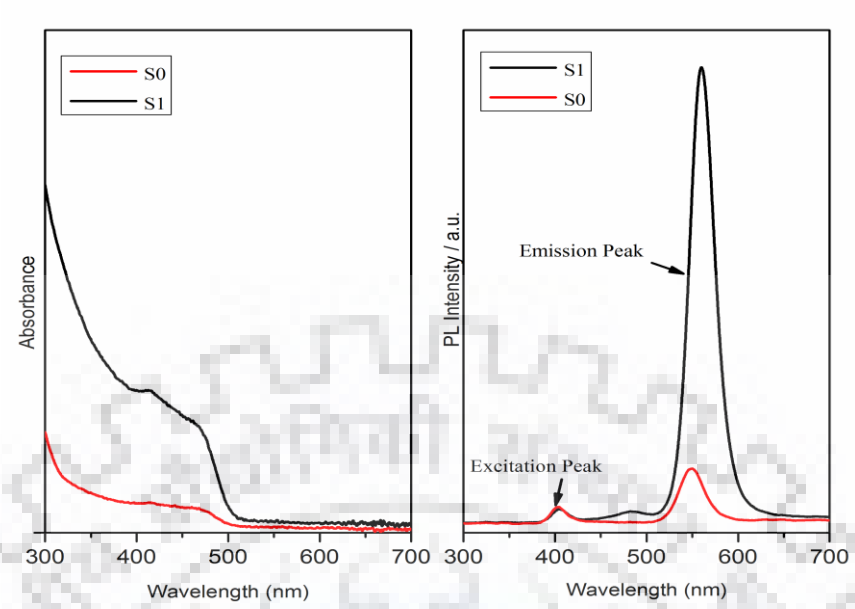

Figure 2.1: Absorbance and PL of CdSe quantum dots sample S0 and sample S1

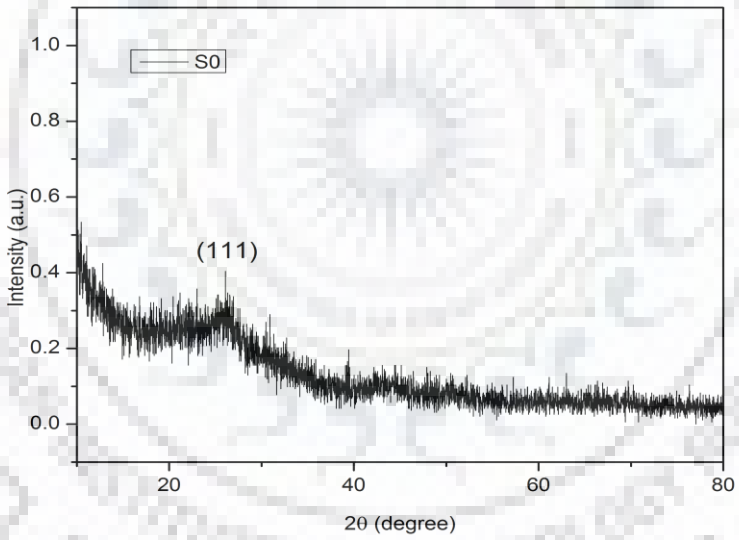

Figure 2.2 XRD of sample S0

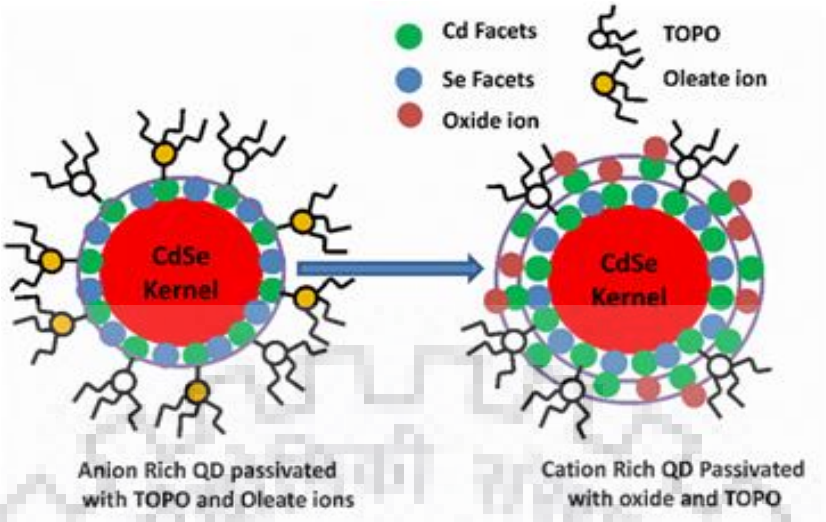

Figure 2.3: Schematics for the conversion of Se rich to Cd-rich QD and further passivation by atmospheric oxygen

The elemental analysis of CdSe QDs was carried out by XPS. Figure 2.5 (a), (b), (c), and (d) and Figure 2.6 shows the XPS spectra of CdSe thin film. In XPS spectra two peaks are observed at 405.0 eV and 411.8 eV corresponding to Cd 3d and peaks in between binding energies 52.00 eV to 56.00 eV correspond to the Se 3d. This elemental study shows a very close resemblance with the XPS spectra of the bulk CdSe. the ratio of XPS integrated peaks for the surface and inner core separated by a few tenths of an eV, a ratio of surface atoms to inner core atoms can be determined [17].

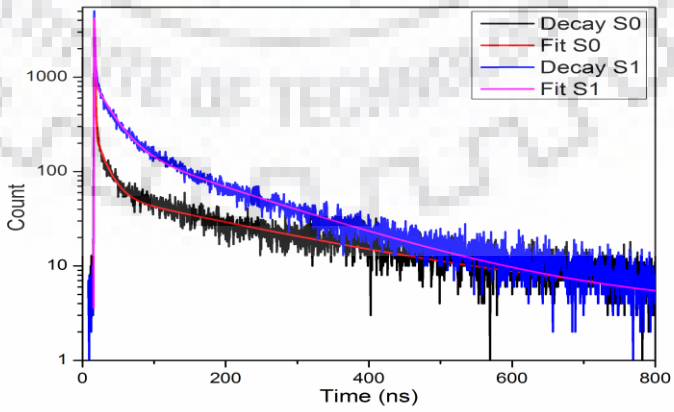

Figure 2.4: Time-resolved PL decay curves of samples S0 and S1

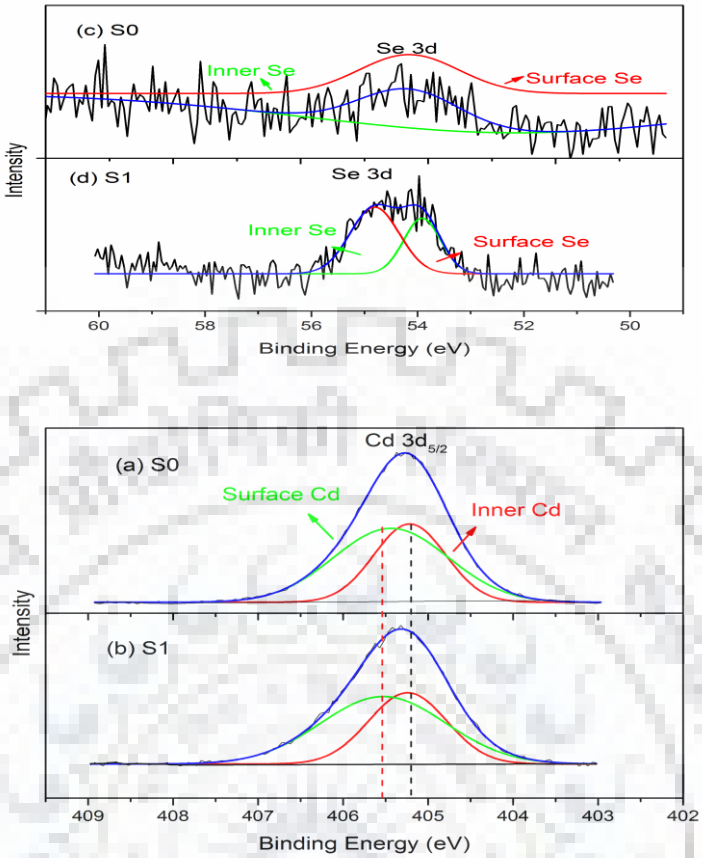

Figure 2.5: XPS spectra and elemental analysis; (a) Cd 3d sample S0 (original) (b) Cd 3d sample S1 (surface treated) (c) Se 3d sample S0 (original), and (d) Se 3d sample S1 (surface treated): Peak analysis of Cd 3d, Se 3d showing inner and surface contributions.

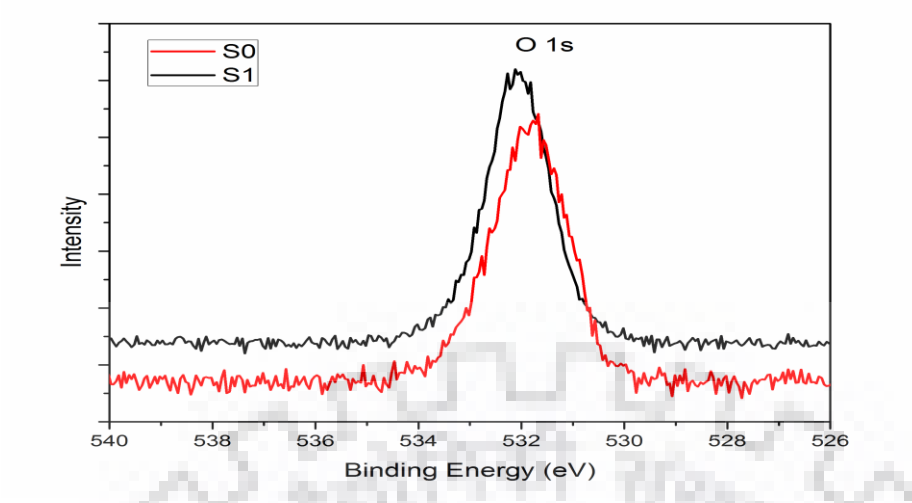

Figure 2.6: XPS spectra of sample S0 (original) and S1 (surface treated); O 1s

As surface defects of QDs are determined by uncoordinated atoms. XPS is the technique to distinguish surface atoms from inner core (kernel) atoms, as they possess different energies in XPS spectra. Taking The ratio of the number of atoms present at surface to the inner core of Cd and Se for samples S0 and S1 summarized in Table 2.2, is obtained from proper peak analysis as shown in Figure. The multi-peaks were obtained and analyzed via deconvolution using the Gaussian fitting procedure. It is clear that the amount of Cd at the surface increases and that of Se decreases after treatment. Also from absorbance and PL analysis of QD, size for S1 is greater than S0 by the atomic size of Cd. Thus it gets justified that there is the formation of new CdSe bonds after treatment with $NaBH_4$ via conversion of Se rich QD to Cd-rich QD. In the original sample, S0 the binding energy of O 1s level was 531.7 eV, which was due to the formation of an oleate bond with a metal ion (i.e. Cd). After treatment, the peak at 532.21 eV and 530.5 eV appearing in Figure 2.6 sample S1, shows the hydroxyl and oxide bonds with cadmium, which confirms the passivation of surfactants in Cd-rich CdSe QD through oxidation. Also, nonappearance of the peak at 531.7 eV in sample S1 confirms the reduction of Cd-O- bond (came from oleate) after the treatment.

It can be concluded that treatment with the NaBH4 oxidized QD surfaces. Initially, it reduces some of the oleate ions surfactants. This causes the facets to lose their coordination properties and come out from the QD caused oxidation of QD surfaces. Initially, it reduces some of the oleate ions surfactants. This causes the facets to lose their coordinating properties and come out of the QD solution forming a monoatomic layer of cadmium. Eventually, oxygen reacts with cadmium to form a CdO layer around the CdSe

QD. Enhancement in quantum yield of QD is observed because the CdO layer passivates the surface defects very effectively and it has no effect on already passivated surface defects by trioctylphosphine (TOP).

In a nutshell, we have converted the Se rich CdSe surfactants QD into Cd-rich QD the quantum efficiency of CdSe QDs considerably by converting Se rich to Cd-rich via a simplified surface treatment using NaBH4, which increases the QY manyfold. This methodology may provide a simple and general scheme to enhance the quantum yield to a large extent with a slight increment in size, and explored in depth the cause of increment in QY.

3. IMPROVEMENT IN QUANTUM YIELD OF BLUE COLOR CdS/CdZnS CORE/SHELL QUANTUM DOTS

In the core structure of quantum dots, quantum yield is limited by non-radiative recombination of electron-hole pairs or excitons. This is due to the presence of surface states created by dangling bonds and other dislocations assisted energy states. The surface passivation of dangling bonds is the main challenge to improve the quantum yield. There are there two popular methods of surface passivation one is organic capping passivation and the other is inorganic passivation. Organic capping passivation is used for the passivation of dangling bonds of core quantum dots. Also, there is an instability problem with organic ligand passivation. To improve the quantum yield with better stability inorganic passivation is preferred that is the synthesis of core/shell structured quantum dots. Inorganic passivation is accompanied by the shelling of core by an inorganic material layer having a higher energy gap than that of the core [18]. The quantum yield (QY) of these quantum dots depends on two factors namely the passivation of surface states of core and thickness of the shell. With the increase in shell thickness, the possibility of misfit dislocations increases. Consequently, there is a generation of extra surface states in between the discrete energy states of quantum dots resulting non-radiative quenching of electron-hole pairs or excitons and hence there is a decrease in quantum yield (QY). From the literature review, it is observed that the quantum yield of quantum dots with CdS as a core, is optimum when shell thickness is about two molecular layers. Assuming that at a given nucleation time and specific fixed temperature, the passivation of dangling bonds has reached to its optimum state. We can now optimize the thickness of the shell to improve the quantum yield. In this work, the same has been demonstrated. By decreasing the shell thickens quantum yield is increased from 12% to 45%.

3.1 Experimental

3.1.1 Materials used: Cadmium oxide (CdO), Zinc acetate ($Zn(OAc)_2.2H_2O$), Sulfur powder (S), Stearic acid (SA), and 1-octadecene (1-ODE) were purchased from Sigma-Aldrich. Acetone and chloroform used were of spectroscopy grade. All materials have purity above 90%.

3.1.2 Synthesis of quantum dots

The CdS/CdZnS blue QDs were synthesized using single step non-injection technique. The sample S0 (say) is prepared by mixing Cadmium oxide (CdO), Zinc acetate ($Zn(OAc)_2$), Sulfur (S), and stearic acid (SA) in molar ratio of 2:1:1:4 with 20 ml of 1-ODE in a 100 ml three necked round flask. The mixture was exposed with compressed air with the vigorous stirring followed by a slow increment of mixture temperature to 260 °C in steps of $20^{O}C$/min. we have collected the sample at 20 min and cooled the flask under the water tap immediately. The sample S1(say) was prepared using the same technique with some modifications including (i) replacement of Zinc acetate by dehydrated Zic acetate and (ii) cooling the QD sample at $0^{O}C$ by putting the flask in the refrigerator for 15 minutes. The samples were purified by mixing it with acetone and chloroform (3:1) and centrifuged at 6000 rpm for 8 min.

3.1.3 Characterization

X-ray thin film diffraction (XRD) patterns of thin film CdS/CdZnS quantum dots were recorded using Bruker, D8-Advance XRD system. Ultraviolet-visible absorbance spectra of QD samples were recorded with a USB: 4000 ocean optics spectrometer assembly. Steady-state photoluminescence (PL) were collected on USB: 4000 ocean optic spectrometer, an LED source (373 nm, FWHM~15 nm) was used as a source of excitation. The quantum yield (QY) of the samples was measured using the integrating sphere equipped with the LED source (373 nm, FWHM~15 nm) and USB: 4000 Ocean spectrometer assembly.Spectra were taken as a standard. Time-correlated single photon counting curves (TCSPC), to measure the lifetime of QDs, were obtained using Fluorescence Lifetime Microscope (HORIBA JOBIN YVON Model-FLUOROCUBE), consisting of nano LEDs with wavelength 373 nm as source of excitation, fluorescence detection range 300 – 800 nm (using TBX-04D detector) and Emission Mono-chromator of range 200 – 850 nm with varying bandwidths in between 1-32 nm in different steps.

Different measurements including absorbance, photoluminescence quantum yield (QY), X-ray thin film diffraction (XRD) patterns, and FLS are performed to justify the results.

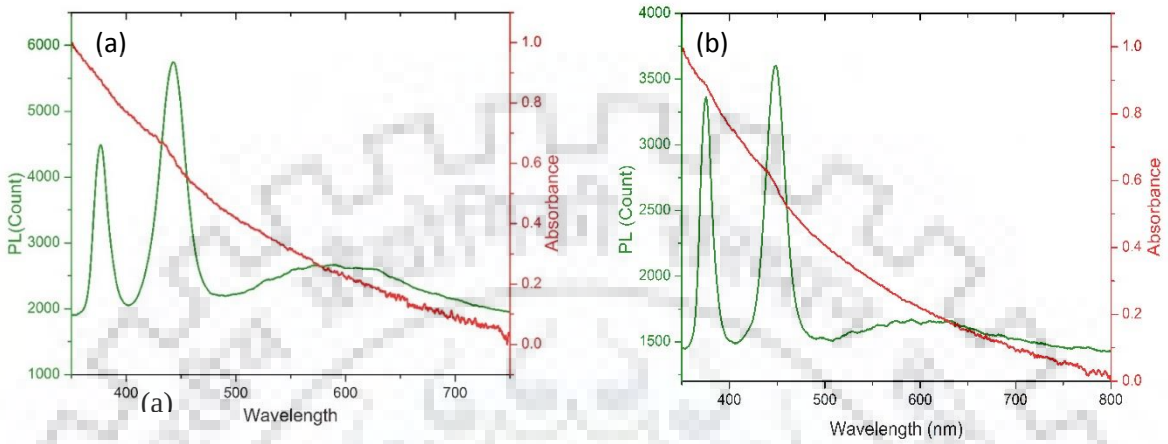

Figure 3.1: Absorbance and PL of CdS/CdZnS core/shell quantum dots(a) sample S0 (b) sample S1

3.2 Results and Discussion

The absorbance and PL characteristics of QD samples S0 and S1 are shown in Figure3.2.

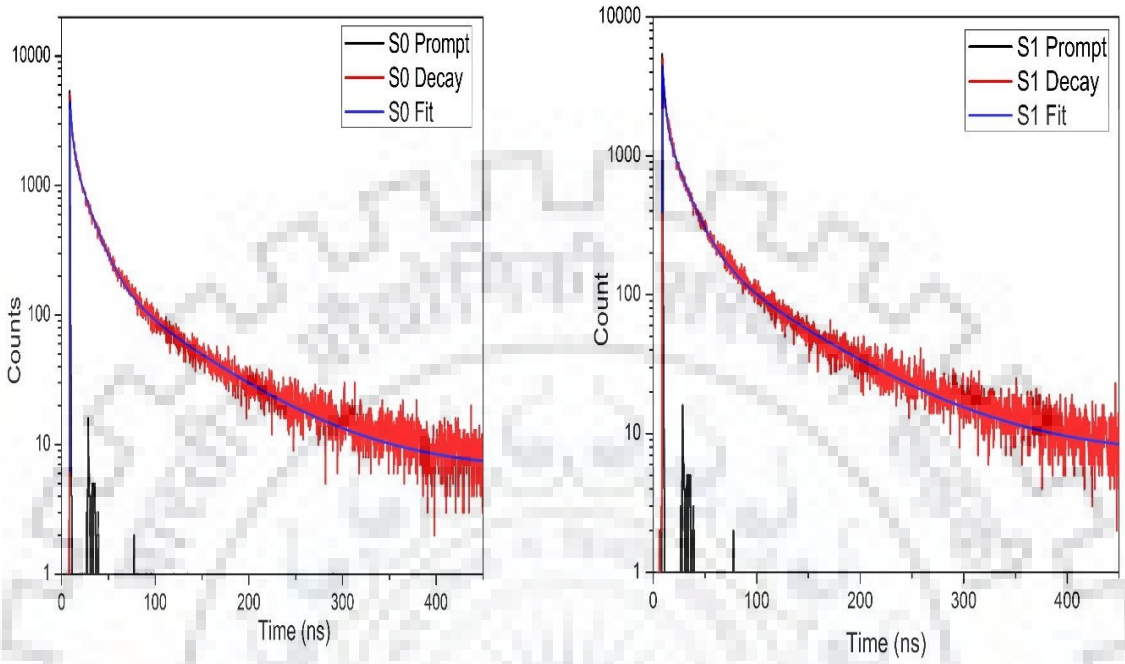

Figure 3.2: FLS of (a) sample S0 (b) sample S1

The fluorescence lifetime of the quantum dots was measured by a time-resolved Fluorescence lifetime measurement setup (Horiba Jobin-Yvon, model-Fluorocube), the excitation wavelength is set to 373 nm. Lifetime measurement is done by fitting the plot with a triple exponential function given by (16).

$$I(t) = A_1\exp(t/\tau_1)+A_2\exp(t/\tau_2)+A_3\exp(t/\tau_3) \quad (16)$$

Here A_1, A_2, A_3 are pre-exponential factors and τ_1, τ_2, and τ_3 are corresponding lifetimes. The average life (τ_{av}) is obtained as the weighted average of τ_1, τ_2, and τ_3 and is given by equation (17) [9].

$$\tau_{av} = (\tau_1 A_1+\tau_2 A_2+\tau_3 A_3)/(A_1+A_2+A_3) \quad (17)$$

The average lifetime of S0 is found about 10.04 nS while that of S1 is 12 nS this increase in lifetime confirms that in sample S1 there is a lesser number of defect states are times greater than that of S0 (2.21 ns). The average lifetime is the function of radiative recombination rate (k_r) and non-radiative recombination rate (k_{nr}) as given by equation (18)

$$\tau_{av} = 1/(k_r+k_{nr}) \quad (18)$$

This increment in the average lifetime of sample S1 is due to decrement in the value of non-radiative recombination rate (K_{nr}) which is direct evidence of decrement of misfit dislocations of the shell.

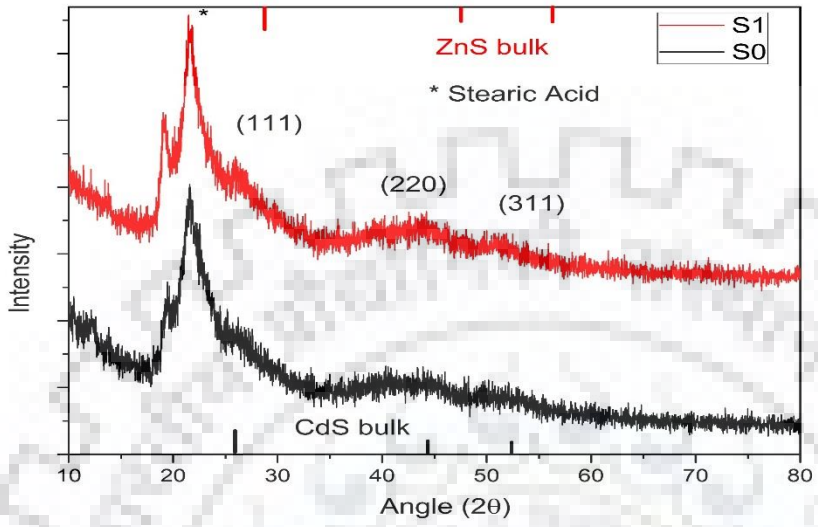

Figure 3.3: X-ray diffractogram of CdS/CdZnS core/shell quantum dots samples S0 and S1

X-ray diffractogram of two samples is shown in the figure 3.3. The sharpness and clearness of peaks at planes (111), (200) and (311) of sample S1 in comparison to that of S0 suggests that sample S1 is more crystalline sample S0. Thus it is clear that sample S1 has fewer misfit dislocations which result in a lesser number of non-radiative deactivations resulting in an increase in quantum yield from 12% to 45 %.

4. FABRICATION AND CHARACTERIZATION OF ORGANIC LIGHT EMITTING DEVICES (OLEDs) AND QUANTUM DOT LIGHT EMITTING DEVICES (QDLEDs)

The processes to fabricate of organic LEDs and quantum dot LEDs are already discussed in chapter 1.We have plenty of material to choose for different layers to ensure the band alignment so as to allow easy transport of charge carriers. The factors influencing, to follow the particular process or material, are ease and good quality deposition of different layers, cost and consumption of time, etc. The Quantum dots are used in QDEDs, as emissive layer. Blue color CdS/CdZnS quantum dots are used in fabrication of QDLEDs.

4.1 Fabrication and characterization of organic light emitting devices (OLED)

Fabrication of Organic Light Emitting Devices (OLED) involves simple processes including Substrate preparation, Fabrication (deposition of different organic and metallic layers) and Packaging.

(a) Substrate preparation: The substrate used is ITO coated glass, which is of very little roughness and the conducting layer of ITO has resistivity less than 10 ohm-cm. Before going to fabricate different layers on the substrate it should be properly cleaned and annealed.

(i) The substrate is cleaned with DI (deionized) water, acetone, and Isopropyl alcohol through sonication for 5 minutes for each in succession.

(ii) Now the substrate is placed in ozonizer. It is firstly heated with nitrogen purging for 5 minutes at 60^{o}C then ozonized for 20 minutes to remove the impurities contaminated at the ITO surface.

(b) Fabrication of OLEDs: This involves the deposition of different layers over the ITO (Indium tin oxide) coated glass substrate.

(i) Deposition of HIL: PEDOT: PSS (poly(3,4-ethylene dioxythiophene)

polystyrene sulphonate) is used to a hole transport layer. It is spin coated at 3500 rpm and annealed for 30 minutes at170^{o}C.

(ii) Deposition of HTL (Hole transport layer): PVK(polyvinyl carbazole) is used as a hole transport layer. It is spin coated at 4000 rpm annealed for 20 minutes at120^{o}C.

(ii) Deposition of Emissive and Electron transport layer: we have used Alq3 which acts as EL and ETL both. Alq3 has deposited through thermal evaporation with a thickness of 45 nm.

(iv) Deposition of Metallic contact: Al is used as metallic contact to work as a cathode in the device. It is deposited via thermal evaporation with a thickness of 250 nm.

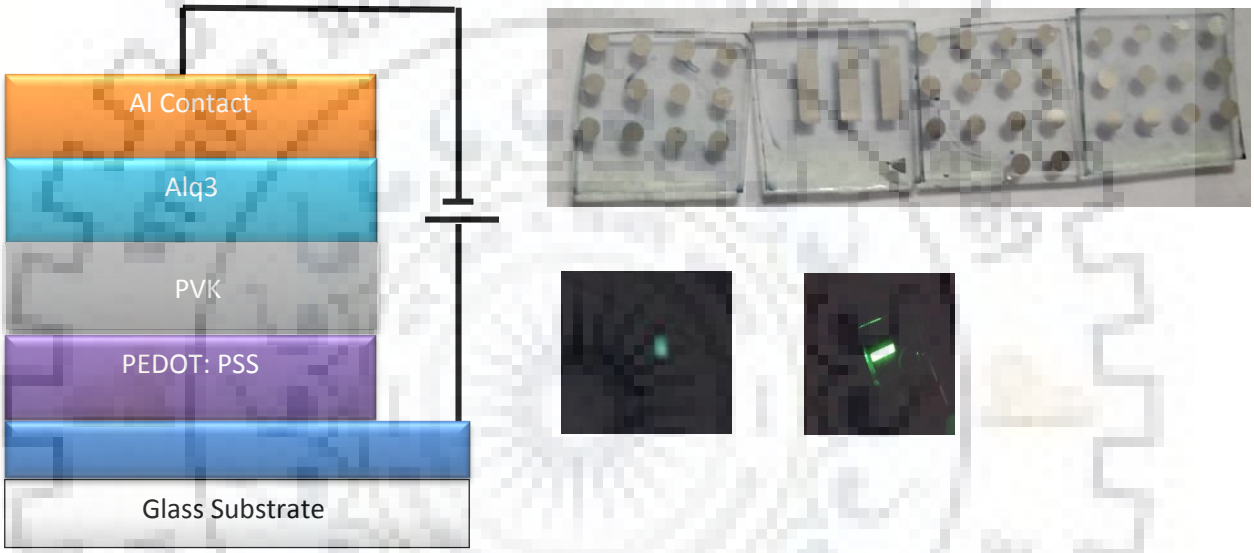

Figure 4.1: Structure of OLED fabricated and glowing of the device

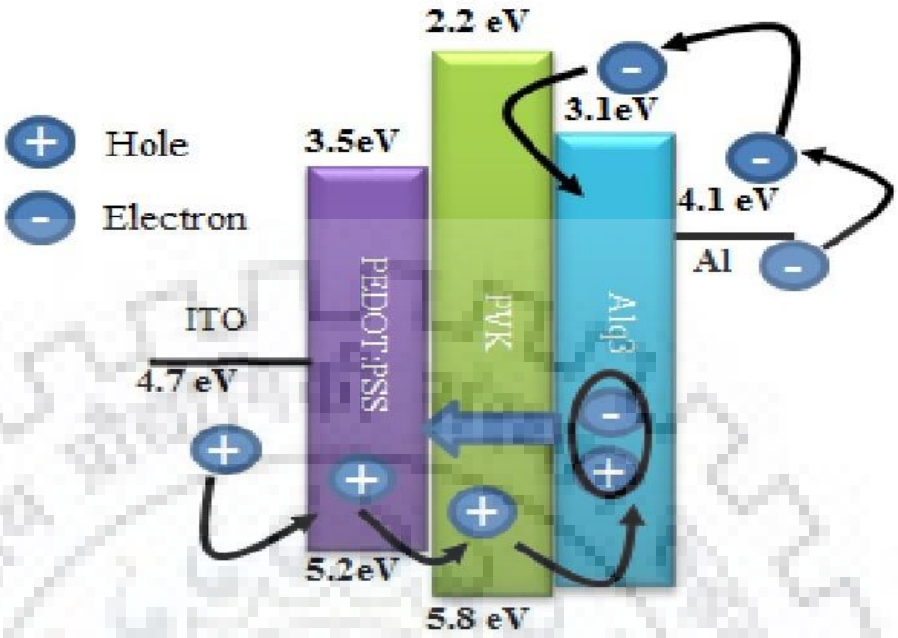

Figure 4.2: Light emission mechanism of OLED fabricated

(c) Characterization: The fabricated devices are probed with the probe station in the lab. Four devices were fabricated with PEDOT: PSS layers at 3500 rpm for each and PVK at 2500, 3000, 3500 and 4000 rpm respectively. There are various instruments namely parameter analyzer, probe station, power meter, and USB: 4000 Ocean spectrometer. Applied voltages are swept across the device electrodes through a parameter analyzer to obtain current density. Current flowing through the device is measured from current density and the known area of the aluminum contacts. Power meter detects the output power and the spectrometer is used to plot the electroluminescence (EL) of the device, for there is a provision of an optical detector in the probe station.

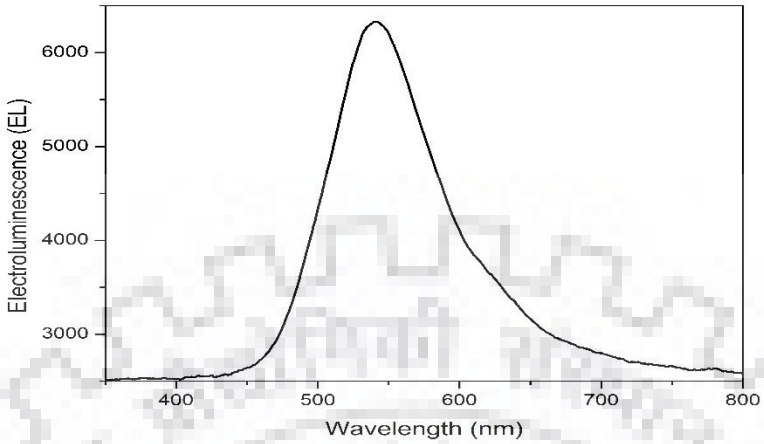

Figure 4.3: Electroluminescence of OLED

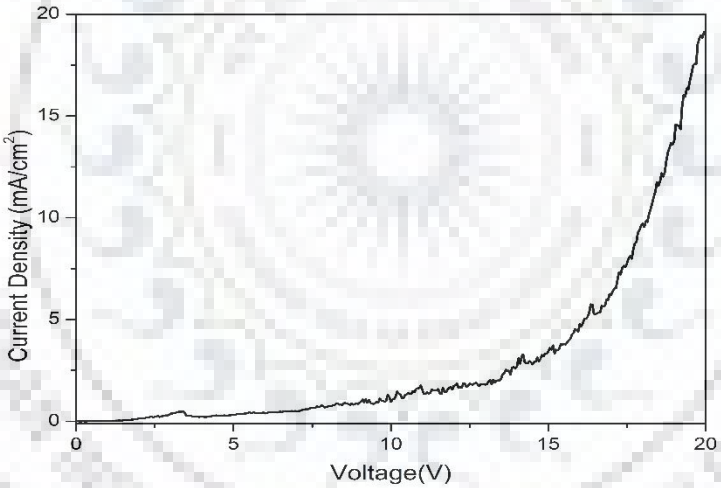

Figure 4.4: J-V characteristic of OLED

Electroluminescence plot shows a peak at 550 nm which is characteristic of green color the same is reflected in the glow of OLED. J-V characteristic shows cut-in voltage at about 10 V.

4.2 Fabrication and characterization of Quantum Dot Light Emitting Devices (QDLEDs)

Fabrication of Quantum Dot Light Emitting Devices (OLED) involves simple processes including Substrate preparation, Fabrication (deposition of different organic and metallic layers) and Packaging.

(a) Substrate preparation: The substrate used is ITO coated glass, which is of very little roughness and the conducting layer of ITO has resistivity less than 10 ohm-cm. Before going to fabricate different layers on the substrate it should be properly cleaned and annealed.

(i) The substrate is cleaned with DI (deionized) water, acetone, and Isopropyl alcohol through sonication for 5 minutes for each in succession.

(ii) Now the substrate is placed in ozonizer. It is firstly heated with nitrogen purging for 5 minutes at 60^{o}C then ozonized for 20 minutes to remove the impurities contaminated at the ITO surface.

(b) Fabrication of QD-LEDs: This involves the deposition of different layers over the ITO (Indium tin oxide) coated glass substrate through spin coating [19].

(i) Deposition of HIL: PEDOT: PSS (poly(3,4-ethylene dioxythiophene)

polystyrene sulphonate) is used to a hole transport layer. It is spin coated at 3500 rpm.

(ii) Deposition of HTL(Hole transport layer): PVK(polyvinyl carbazole) is used as a hole ransport layer. It is spin coated at 4000 rpm.

(iii) Deposition of Emissive and Electron transport layer: we have used blue CdS/CdZnS quantum dots which acts as an emissive layer.

(iv) Deposition of Metallic contact: Al is used as metallic contact to work as a cathode in the device. It is deposited via thermal evaporation with a thickness of 250 nm.

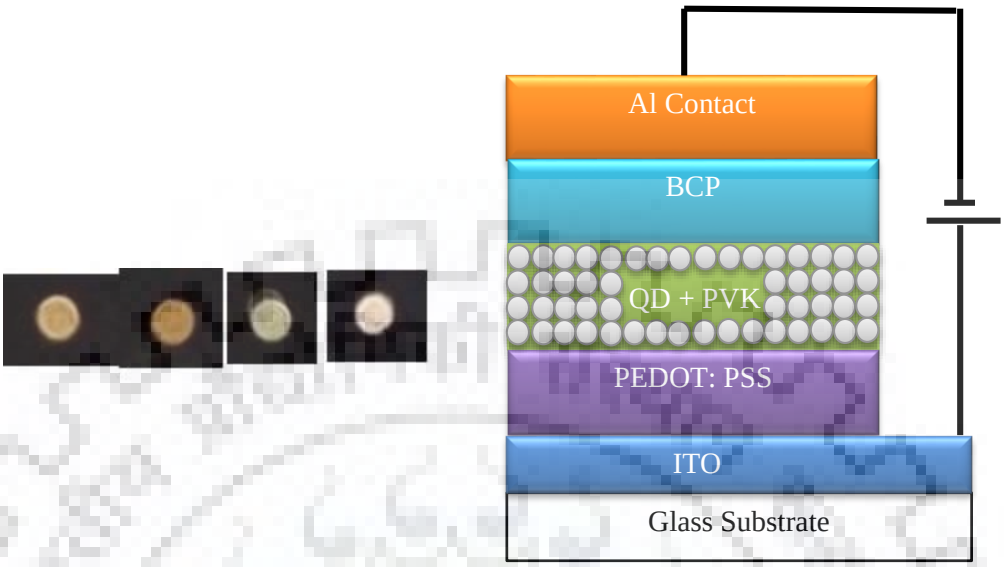

Figure 4.5: Structure of QDLED fabricated and glowing of the device showing warm white color

(b) Characterization

Characterization includes mainly the plots of J-V characteristic, EL measurement, and efficiency calculations.

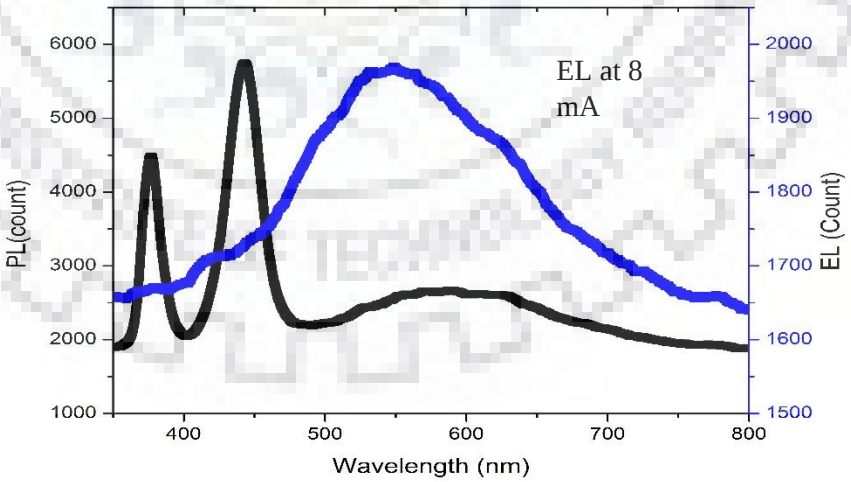

Figure 4.6: EL and PL of QDLED

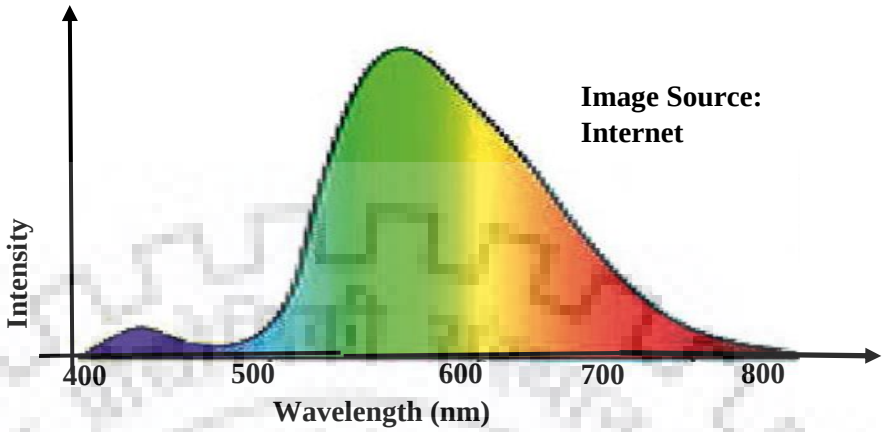

Figure 4.7: PL of warm white light

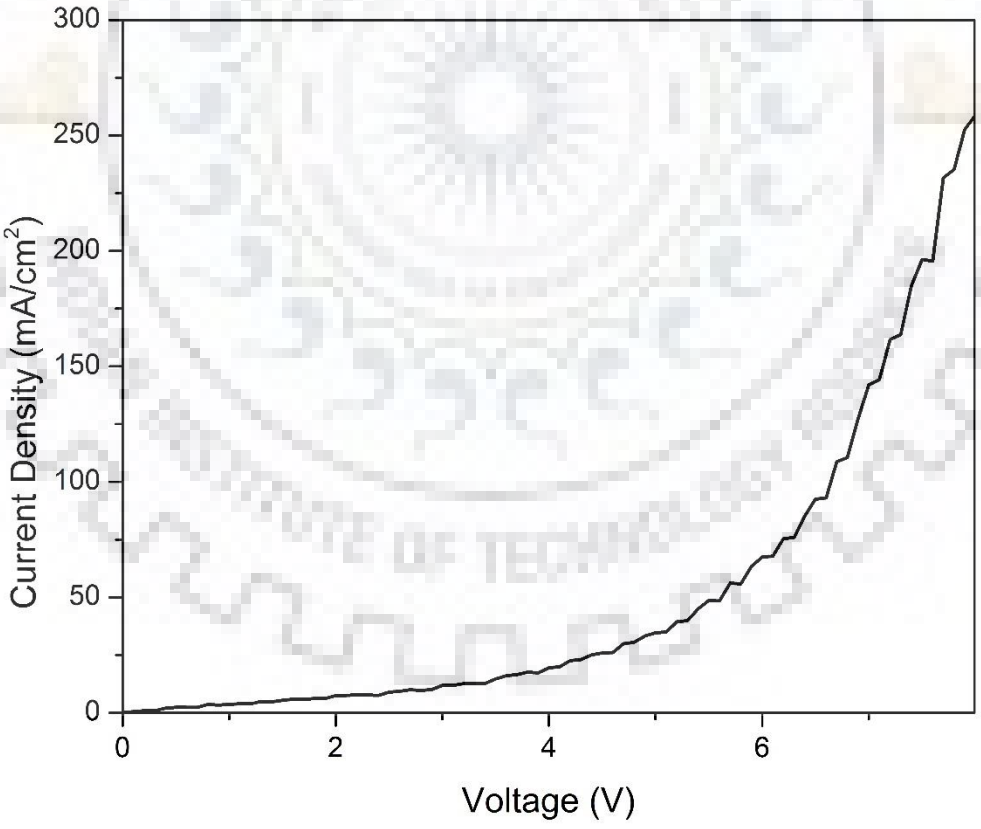

Figure 4.8: J-V characteristics of QDLED

From J-V characteristics it is clear that the cut-in voltage of the QDLED fabricated is about 5V. Also, the device size of 2mm diameter so the maximum current flows through the device is about 10 mA. The EL is found at a constant current of 8 mA as shown in the characteristic plot. It is clear that the El of OLED has a close resemblance with the spectra of warm white light.

5. CONCLUSION AND SCOPE OF FUTURE WORK

5.1 Conclusion

A literature survey of quantum dot and quantum dot light emitting devices was carried out. The survey includes different ways of synthesis of quantum dots, techniques to improve the quantum yield of CdSe and CdS/CdZnS quantum dots and their characterization. Quantum yield of CdSe quantum dots was improved from 1.52% to 16.03% while that of blue CdS/CdZnS core-shell quantum dots were improved from 12% to 45%. Different characterizations such as absorbance, PL, FLS, XRD, and XPS were done and results were analyzed to justify this increment of quantum yield. It also includes a detailed study about OLEDs and QDLEDS their different structures, suitable materials that are required to fabricate the device, carrier transport within the device. Also methods of cleaning the substrate, requirement of necessary condition and optimization of spin speeds for different layers of the device so that proper charge transport is allowed resulting successful working of the device. Further, two types of the bottom emitting structure studied in the literature survey have been fabricated in the lab one corresponding to OLED and the other corresponds to QDLED. Also, an attempt for reducing steps in the fabrication of devices is studied this includes the blending effect of Alq3 and PVK, the result was partially successful, this requires more optimization to be succeeded. The characterization of the fabricated OLED showed the green color LED due to the use of Alq3 as an emissive layer and the color of QDLED was warm white color due to the use of blue CdS/CdZnS quantum dots. The EL spectra of QDLED is similar to that of the Alq3 based OLEDs with broadening of the components from 400 nm to 750 nm which results in the warm white glow.

5.2 Scope for future work

As discussed in the previous sections, the lab work done during the project included synthesis of quantum dots, fabrication of simple OLED and QD LED and the study blending effect of the ETL and HTL layers. This also includes methods to improve the quantum yield of CdSe and CdS/CdZnS quantum dots. For all the above, the scope of work can be summarized in the following points.

- The procedure can be used to synthesize quantum dots with higher efficiencies of other kinds of quantum dots.
- The work can be extended to prepare the PDMS stamp and use it for the printing of quantum dots for QDLED.
- For the static dispense spin coating study, the observation can be modeled into some mathematical formulation by considering the results obtained during the experiments.
- The blending effect of Alq3 and PVK and other ETL and HTL layers can be carried out to reduce the number of steps.

References

[1] P. Kathirgamanathan, L. M. Bushby, M. Kumaraverl, and S. Ravichandran, "Electroluminescent Organic and Quantum Dot LEDs : The State of the Art," vol. 11, no. 5, pp. 480–493, 2015.

[2] W. Brütting, J. Frischeisen, T. D. Schmidt, B. J. Scholz, and C. Mayr, "Device efficiency of organic light-emitting diodes: Progress by improved light outcoupling," *Phys. Status Solidi Appl. Mater. Sci.*, vol. 210, no. 1, pp. 44–65, 2013.

[3] B. Kumar, *CHARGE TRANSPORT IN QUANTUM DOT – LIGHT EMITTING DEVICES*, no. August. 2013.

[4] Y. Wang and N. Herron, "Nanometer-sized semiconductor clusters: Materials synthesis, quantum size effects, and photophysical properties," *J. Phys. Chem.*, vol. 95, no. 2, pp. 525–532, 1991.

[5] E. Kuçur, W. Bücking, R. Giernoth, and T. Nann, "Determination of defect states in semiconductor nanocrystals by cyclic voltammetry," *J. Phys. Chem. B*, vol. 109, no. 43, pp. 20355–20360, 2005.

[6] A. D. Yoffe, "Semiconductor quantum dots and related systems: Electronic, optical, luminescence and related properties of low dimensional systems," *Adv. Phys.*, vol. 50, no. 1, pp. 1–208, 2001.

[7] L. E. Brus, "A simple model for the ionization potential, electron affinity, and aqueous redox potentials of small semiconductor crystallites," *J. Chem. Phys.*, vol. 79, no. 11, pp. 5566–5571, 1983.

[8] karuna kar nanda and J. Khatei, "quantum confinement.pdf." .

[9] A. Nath Bhatt, U. K. Verma, and B. Kumar, "Temporal evolution of white light emitting CdS core and Cd 1-x Zn x S graded shell quantum dots fabricated using single step non-injection technique," *Opt. Mater. (Amst).*, vol. 92, no. January, pp. 143–149, 2019.

[10] A. M. Smith and S. Nie, "Semiconductor nanocrystals: Structure, properties, and band gap engineering," *Acc. Chem. Res.*, vol. 43, no. 2, pp. 190–200, 2010.

[11] E. Jang, S. Jun, Y. Chung, and L. Pu, "Surface Treatment to Enhance the Quantum Efficiency of Semiconductor Nanocrystals," *J. Phys. Chem. B*, vol. 108, no. 15, pp. 4597–4600, 2004.

[12] R. K. Ratnesh and M. S. Mehata, "Synthesis and optical properties of core-multi-shell CdSe/CdS/ZnS quantum dots: Surface modifications," *Opt. Mater. (Amst).*, vol. 64, pp. 250–256, 2017.

[13] W. W. Yu, L. Qu, W. Guo, and X. Peng, "Experimental determination of the extinction coefficient of CdTe, CdSe, and CdS nanocrystals," *Chem. Mater.*, vol. 15, no. 14, pp. 2854–2860, 2003.

[14] F. Wikipedia, "Ionic radius," *Wiki*, pp. 1–10, 1000.

[15] M. T. Man and H. S. Lee, "Interband Transition and Confinement of Charge Carriers in CdS and CdS/CdSe Quantum Dots," *Appl. Sci. Converg. Technol.*, vol. 24, no. 5, pp. 167–171, 2015.

[16] B. Omogo, J. F. Aldana, and C. D. Heyes, "Radiative and nonradiative lifetime engineering of quantum dots in multiple solvents by surface atom stoichiometry and ligands," *J. Phys. Chem. C*, vol. 117, no. 5, pp. 2317–2327, 2013.

[17] Y. Ye, X. Wang, S. Ye, Y. Xu, Z. Feng, and C. Li, "Charge-Transfer Dynamics Promoted by Hole Trap States in CdSe Quantum Dots-Ni2+ Photocatalytic System," *J. Phys. Chem. C*, vol. 121, no. 32, pp. 17112–17120, 2017.

[18] W. Ki Bae *et al.*, "Deep blue light-emitting diodes based on Cd1-xZn xS@ZnS quantum dots," *Nanotechnology*, vol. 20, no. 7, 2009.

[19] P. Yimsiri and M. R. MacKley, "Spin and dip coating of light-emitting polymer solutions: Matching experiment with modelling," *Chem. Eng. Sci.*, vol. 61, no. 11, pp. 3496–3505, 2006.